PLASTIC TORSIONAL BUCKLING OF THIN WALLED CIRCULAR CYLINDERS

A MASTER THESIS

SUBMITTED TO THE DEPARTMENT OF MECHANICAL ENGINEERING
AND THE COMMITTEE ON THE FACULTY OF ENGINEERING AT GAZİANTEP
OF MIDDLE EAST TECHNICAL UNIVERSITY
IN PARTIAL FULFILLMENT OF THE REQUIREMENTS
FOR THE DEGREE OF
MASTER OF SCIENCE

By

Zarif ÜNAL

February 1984

I certify that I have read this thesis that in my opinion it is fully adequate, in scope and quality, as a thesis for the degree of Master of Science.

Supervisor

Prof.Dr.Alp ESİN

I certify that this thesis satisfies all the requirements as a thesis for the degree of Master of Science.

Chairman of the Department

Assoc.Prof.Dr. Ömer T.GÖKSEL

Examining Committee in Charge :

S.Süleyman SARITAŞ	S.Laptaş
İ.Hüseyin Filiz	H.Filiz
A.İhsan SÖNMEZ	
Can Akkoş	Akkoş

Committee Chairman

ABSTRACT

PLASTIC TORSIONAL BUCKLING OF
THIN WALLED CIRCULAR CYLINDERS

ÜNAL, Zarif
M.S. in Mechanical Engineering
Supervisor: Prof. Dr. Alp Esin
February 1984 , 83 Pages.

A thin-walled cylindrical shell subjected to a twisting moment about its longitudinal axis (pure torsion) exhibits plastic buckling if the material of the shell is ductile. Although the problem of elastic buckling has been investigated and substantial data is available in literature, plastic buckling of shells has not been treated as throughly.

The present work is directed toward a mathematical formulation of the plastic buckling problem. In particular, the torque for plastic buckling is predicted for thin-walled cylinders of different materials and dimensions. A computer program for evaluation of the theoretical model is developed and the results compared with those obtained from experiments.

It has been shown that the proposed equation to predict the torsional buckling of thin-walled cylinders is in good agreement with the experimental results. The suggested analytical method is simple in form and the relevant parameters could easily be determined by simple mechanical tests. The

proposed method is therefore highly practical and is much more convenient than a method based on limit analysis.

Key Words : Torsional buckling, Thin-Walled cylinders.

ÖZET

BURMA MOMENTİ UYGULANMIŞ İNCE CİDARLI DAİRESEL KESİTLİ SİLİNDİRLERİN PLASTİK BURKULMASI

ÜNAL, Zarif
Yüksek Lisans Tezi, Makina Mühendisliği Bölümü
Tez Yöneticisi : Prof.Dr.Alp ESİN
Şubat 1984, 83 Sayfa.

Simetri ekseni etrafında burma momentine (tork) tabi tutulan ince cidarlı bir boru, malzemesi sünek olursa plastik burkulmaya uğrar. Her ne kadar elastik burkulma konusu oldukça araştırılmış ve literaturde bu konuda yeterince kaynak bulunabiliyorsa da, plastik burkulma yeteri kadar ele alınmamıştır.

Bu çalışma plastik burkulma probleminin matematiksel formülasyonu ile ilgilidir. Geliştirilen bu matematik modelle, malzemeleri farklı ve değişik ölçülerdeki ince cidarlı silindirlerin plastik burkulması için gerekli tork hesaplanabilmektedir. Teorik modelin değerlendirilmesi için bir bilgisayar proğramı hazırlanmış ve elde edilen sonuçlar deneysel sonuçlarla karşılaştırılmıştır.

İnce cidarlı silindirlerin plastik burkulması için geliştirilen modelden elde edilen sonuçlar ile deneysel sonuçlar yakından uyumludur. Önerilen analitik metodun kullanımı basittir ve ilgili parametreleri kolayca çekme deneyinden elde edilebilir. Bu nedenden dolayı sunulan metod

oldukça kullanışlı ve bu tür problemler için Limit Analiz Metoduna göre daha uygundur.

Anahtar Kelimeler : Burma burkulması, İnce Cidarlı Silindirler.

ACKNOWLEDGEMENTS

I would like to express my deepest gratitude to Prof.Dr.Alp Esin for his patient supervision, valuable guidance, criticism and helpfull encouragements throughout this thesis.

I wish to express sincere thanks to Dr.A.İhsan Sönmez for his helpfull suggestions and comments.

The computer program was run at the Computer Center of the University of Fırat. I am obliged to the authorities for making the facilities avialable and would also like to express my sincere appreciation for the courtesy extended: and the assistance rendered by my colleagues Bülent Tutak and Bahri Uzuner.

I am in appreciation of the care exercised by Mr.Ökkeş Yıldırım and Mr.Yaşar Korkutan in the preparation of the specimens.

Finally, thanks are also extended to Miss Ruhat Doğantan for her painstaking efforts and care in typing the manuscripts.

TABLE OF CONTENTS

LIST OF TABLES

LIST OF FIGURES

NOMENCLATURE

A	Constant in empirical Swift's expression related to the basic strength of the material
a	Major axis of the ellipse
B	Constant in empirical Swift's expression related to the initial state of the material
b	Minor axis of the ellipse
C_s	Non-dimensional stress coefficient
D	Outside diameter of the cylinder
d	Inside diameter of the cylinder
E	Young's modulus
$\overline{E}$	Double modulus
E_r	Reduced modulus
E_s	Secant modulus
E_t	Tangent modulus
G	Shear modulus
h	Ordinate of the development curve of the ellipse
I	Second moment of area of the cross section
K	Multiplication factor for effective length
k_s	Modification factor for critical buckling stress equation
k_t	Non-dimensional critical stress coefficient
L	Gauge length of the cylinder
l	Critical column length
n	Number of waves in circumferential direction
P_{cr}	Critical buckling load in Euler equation
P	Peripherial length
R	Mean radius of the cylinder
$\overline{R}$	Distance between the dial gauge plunger axis and the axis of the cylinder
r	Radius of the elastic core on circular cylinder cross section

S	arc length
T	Applied torque
t	Cylinder wall thickness
u,v,w	Displacements measured in the radial, circumferential, and axial directions
x,y	Cartesian coordinates on the plane of cut
Y	Yield stress
y_1	Distance of elastic-plastic boundary along the thickness of the cylinder
r,θ,z	Cylindrical coordinates in radial, tangential, and axial directions of the cylinder
ρ,β',z'	Cylindrical coordinates on the plane of cut
Z	Batdorf parameter $(Z = \frac{L^2}{Rt}(1-\nu^2)^{1/2})$
γ	Correlation factor
η	Plasticity correction factor
ν	Poisson's ratio
α	Angle of cut
ρ	Radius of curvature
$\bar{\sigma}, \bar{\varepsilon}$	Equivalent stress and strain respectively
τ	Pure shear stress
τ_{cr}	Critical buckling stress
σ_1, σ_2	Principal stresses acting along and perpendicular to the helix respectively
$\sigma_{\rho'}, \sigma_{\beta'}, \sigma_{z'}$	Stresses in thickness, tangential and axial directions of the elliptical shell element formed by α - plane.

CHAPTER 1

INTRODUCTION

1.1 General Remarks

In the design of machine parts or structures strength, weight, and cost are the important parameters. In the past, machine parts or structures were clumsy due to the lack of knowledge, technology, and high strength materials; but, later, advents in technology and in industrial areas (eg.aerospace industry) forced the engineers to design lighter but stronger structures.

This has placed a heavy emphasis on the design of high strength-to-weight ratio structures; which in turn has placed a heavier emphasis on the utilization of thin walled members as structural elements.

A variety of machine parts or structures, therefore, consist of or include thin walled cylinders and/or shell panels. Shell is a body bounded by two curved surfaces between which the distance is small compared with the other dimensions. Thin walled cylinder, on the other hand, is a closed form of a shell. Cylinders with relatively small diameter-to-thickness ratios are usually referred to as tubes or pipes whereas cylinders with large diameter-to-thickness ratios are called thin walled cylindrical shells. Cylindrical shells are used as grain storage tanks, pressure vessels, etc.

The thin walled structural elements have introduced special problems of structural instability, which hitherto were not of great concern. On account of this fact, buckling has become one of the main governing factors and a great deal of analytical and experimental work has been

done to investigate the buckling behaviour.

In order to design efficient and reliable structures of which thin-walled members are important components, the engineers must understand the physics of shell buckling to avoid unexpected catastrophic failure.

Buckling is a sudden collapse, involving very large deformation. Contrary to plastic deformation, once buckling starts, it advances till complete failure. Consequently, it is of vital importance to be able to establish the critical conditions that start buckling.

Buckling results from axial compressive stress. However, there are many cases of buckling in which the type of loading could easily delude one to overlook the possibility of buckling. One of such cases is the pure torsion of thin walled cylindrical members. Experience has shown that the buckling failure of thin walled torsional cylinders is equally probable as the acknowledged shear failure, and may even be more prominent in some cases.

Although the buckling failure may take place within the elastic or the plastic range of a metal, it is usually understood as the former. This is on account of the fact that, in most engineering applications the elastic limit of a material is taken as the basis of the load carrying capacity of the member.

When the design efficiency is of paramount importance, if some degree of plastic deformation is permissible and the loads are not of cyclic nature, or if the so called one cycle is very slow or the service life is very short, utilization of the plastic properties of a material is common practice. Under such circumstances, the ultimate strength of the material is taken as the treshold of instability or the termination of the load carrying capacity of the material. However, just like in the elastic

range, a member could fail due to buckling long before the stresses reach the ultimate strength.

Furthermore, it is obvious that when the stresses overshoot the elastic limit, a failure due to plastic buckling is not a remote possibility, and the ductility of the material would not provide an extra margin of safety to the extent implied by the ultimate strength.

It is in above respects that it was found of both theoretical and practical interest to investigate the phenomenon of plastic buckling resulting from the torsion of thin walled cylinders.

1.2 Plastic Buckling Phenomenon

Though ordinary buckling is a well-known type of failure, buckling of thin walled circular cylinders under torsion is difficult to visualize in the face of predominant twisting. For the sake of clarity, and to be able to shed light on the following sections, it was found worthwhile to discuss this type of failure in brief.

When a cylinder is subjected to torsion, the sections are subjected to an angular deformation which results in the twisting of the member. From the classical theories it's a well known fact that, during the twisting action, the elements are subjected to pure shear stresses in transverse planes (Fig.1a). From Mohr's Circle (Fig.1b) these stresses correspond to equal tensile and compressive stresses along the planes which make 45^{o} with the axis of the cylinder (Fig.1c).

The compressive stresses acting on an element A may tend to induce a failure by buckling which proceedes a shear failure if the thickness-to-diameter ratio is small. Just like the shear failure (i.e., plastic flow of the member or complete twist off), buckling may be observed within the elastic limit or before the final

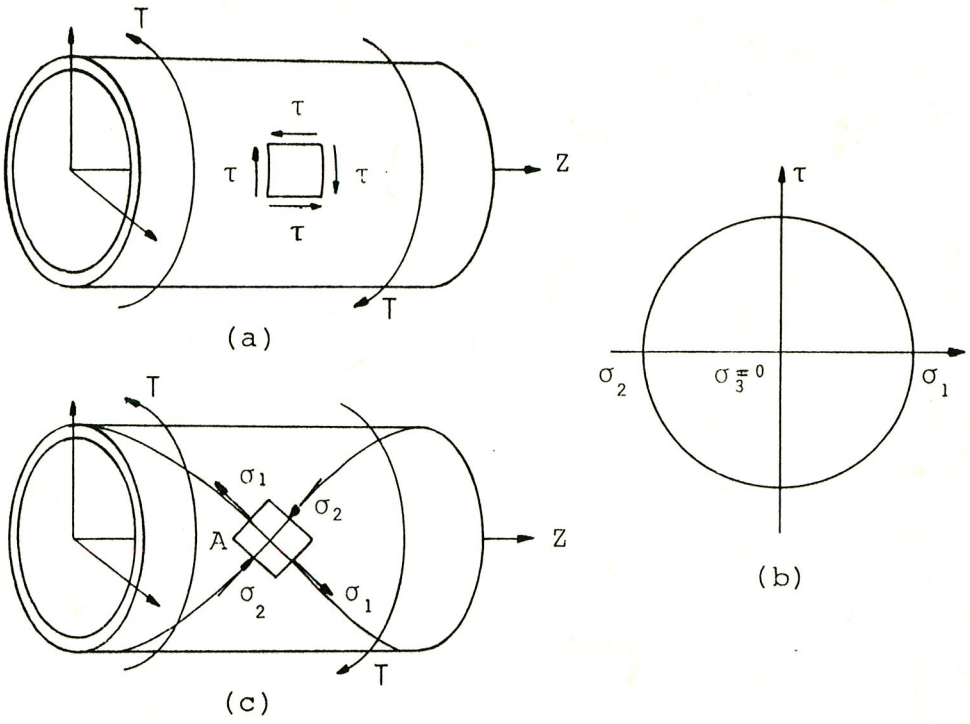

Fig.1 Pure shear due to torsion (a) is equivalent to a biaxial state of equal tension and compression on ± 45° planes (b and c).

rupture; as dictated by thickness-to-diameter ratio.

The buckling failure of a thin cylinder (Fig.2a) in torsion is shown in Fig.2b. One can notice that the form of failure is similar to the collapse of a compressive member. The failure is advanced along an approximately 45° helix. This collapse is termed "a wave" in the relevant literature.

Another interesting aspect of the buckling is the presence of multiple waves at the onset of failure. The general concences of opinion based on different observations is that the number of waves is a minimum of two in elastic buckling.

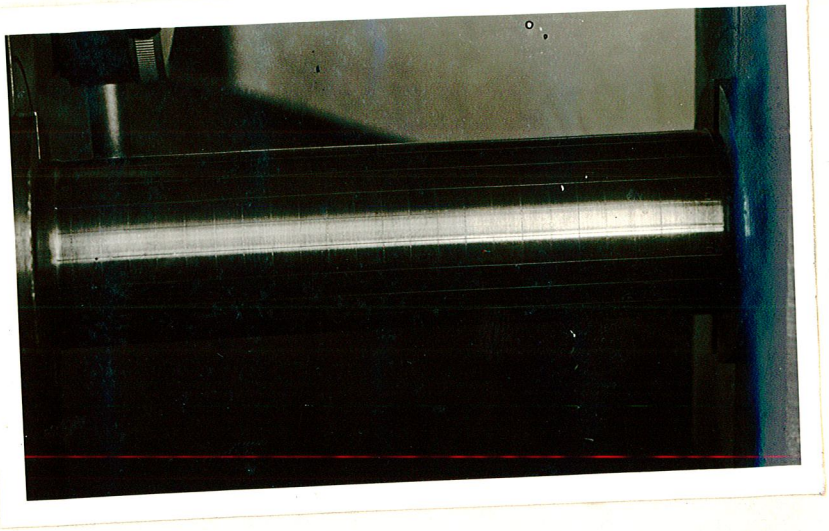

2a- Thin walled circular cylinder before buckling

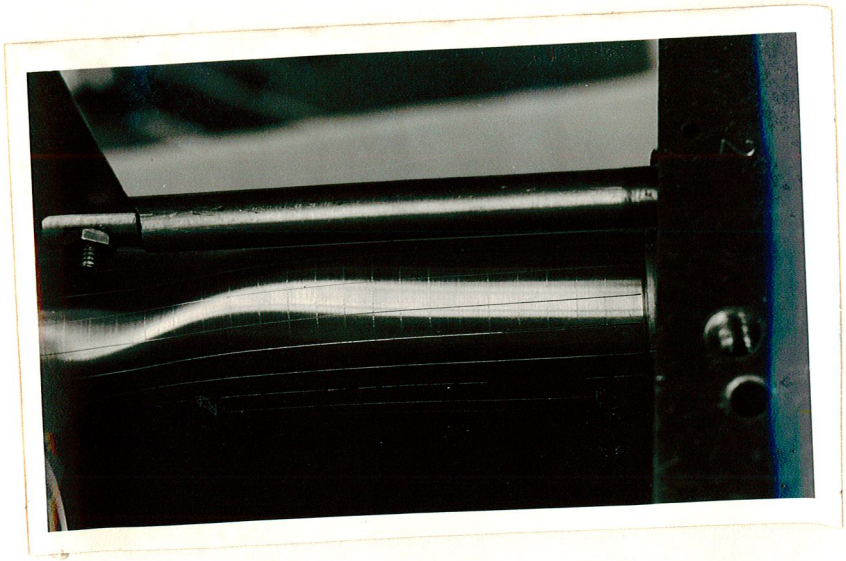

2b- Same tube in Fig.2a after buckling

Fig.2

CHAPTER 2

PREVIOUS WORK ON BUCKLING

2.1 Introduction

Buckling failure of thin walled cylinders under pure torsion has received considerable attention in recent years. Although extensive investigations and voluminous publication have been made on the subject of elastic torsional buckling, plastic buckling of thin walled circular cylindrical shells has not been treated as throughly as the former. In fact, most of the solutions offered are a simple modification of the elastic buckling equations by a constant which is given the name of "Plasticity Correction Factor ".

2.2 Survey on Buckling

Although a theory of shells was first presented in the work of G.Aron [1] , his development was not strictly correct. The inaccuracies in his theory were noticed and corrected by E.H.Love [2], in 1888. He formulated a theory of shells in analogy to the theory of plates of Kirchoff [3]. His set of general shell equations has served generations of authors as the starting point for their work. Love's shell theory was presented in the form most frequently used today by W.Flügge [4] , in 1932. This latter form of shell theory has appeared in the text books by W.Flügge [5] , Bienzo and Grammel [6] , and Timoshenko [7] .

The most comprehensive analysis on the buckling of thin walled cylindrical shells was presented by L.H. Donnell [8] , in 1933. In his work, Donnell proposed a new simplified method of solution utilizing classical,

small deflection shell theory. He formulated the general differential equations for non-linear shell deflection without any simplification except for the use of Love-Kirchoff approximations. These simplifying approximations permit the conversion of the plate or shell problem from three to two dimensional case.

Donnell, then, formulated linear shell equations by discarding the higher order terms in non-linear shell equations, and solved for different boundary conditions and loadings. He formulated the critical buckling stress under torsional loading (Ref.8) for long and medium length of fixed-ended and hinged-ended thin walled circular cylinders.

The prediction of the elastic buckling stress for short and medium length cylinders by Donnell's method has been shown to be greatly in error [9], [10], [11]. On the other hand, it is quite successful when applied to infinitely long cylinders;as has been verified by various authors [10], [11]. However,it is cited [10], [12] that a method has been suggested by Batdorf [13] to extend Donnell's method to the buckling of short circular cylinders.

Unlike Donnell, who started with general equations, Flügge [14] considered different classes of shells and developed the basic equations for each of them separately, employing the same fundamental principles. He formulated differential equations for the disturbed equilibrium of the shell under general basic loadings (i.e., uniform normal pressure on its wall, axial compression and shear load applied at the edges) and solved for any specific type of loading and boundary conditions. He obtained a similar expression for critical buckling stress of a thin walled circular cylinder under elastic torsion as given by equation 27-b of Ref.[15].

In the monograph published by NASA Office of Advanced Research and Techonology [15] , buckling of isotropic unstiffened cylinders, orthotropic cylinders, and sandwich cylinders under various conditions of loadings is given in summary. Torsional buckling of thin walled circular cylinders is considered elastically and plastically, by taking the plasticity correction factor into account.

Baker, Kovalevsky, and Rish [16] summarized several design equations for estimating the collapse loads of thin walled cylinders in various elastic buckling modes as well as interactions between these modes. This book is based on the NASA publication, "Shell Analysis Manual" [17] , and is claimed to be a basic tool for the design of shells. However, C.G.Foster [18] reported an outline of the test results conducted on cylinders loaded in axial compression, hoop compression, torsion and combinations of these as well, and compared his results with the values calculated from Baker, Kovalevsky, and Rish's equations. He pointed out that the results were not in agreement.

Although the simplifications somewhat limit the range of applicability of the Donnell's equations (e.g. for very short cylinders), these equations form the basis for more stability analyses in the literature than any other set of cylindrical shell equations. Applications of the Donnell's stability equations for different loadings were presented by Brush and Almroth [10] . They rederived Donnell's linear and non-linear equilibrium equations for shallow(i.e.,very large radius-to-thickness ratio) and non-shallow cylindrical panels or for complete cylinders. Their solutions are based on Donnell method for long cylindrical shell and conditions of which have little influence on the magnitude of the critical load.

Donnell formula for critical stress at which elastic buckling occurs was also used by D.W.A.Rees [19] . He formulated the critical buckling stress by taking the second order axial strain due to the end conditions into consideration and modified his equation for plastic case by multiplying it by plasticity correction factor. In his work, he approximated the state of pure shear by applying preloads to prevent the accumulation of axial strain.

2.3 Discussion of the Previous Work on Torsional Buckling

In the present development of stability equations for thin walled circular cylindrical shell major emphasis is placed on the relatively simple equations suggested by Donnell in Ref. [8] . As was stated in section 2.2., in the calculation of critical buckling stress, Donnell solutions has formed the basis for most of the other work [10], [11] . Consequently, the equations for the critical buckling stress obtained by these authors are very similar to Donnell's equation (Table-1). He proposed the following relationships between the critical stress and the proportions of the shell, given in Ref. [11] , as :

$$\tau_{cr} = \frac{Et^2[\,4.6 + \sqrt{7.8 + 1.67(\sqrt{1-\nu^2}L^2/2Rt)^{3/2}}\,]}{(1-\nu^2)L^2} \qquad (1)$$

for clamped edges, and

$$\tau_{cr} = \frac{Et^2[\,2.8 + \sqrt{2.6 + 1.4(\sqrt{1-\nu^2}L^2/2Rt)^{3/2}}\,]}{(1-\nu^2)L^2} \qquad (2)$$

for simply supported edges, Where :

E : Young's Modulus

L : Length of the tube

R : Mean radius of the tube

t : Wall thickness of the tube

ν : Poissons Ratio

Donnell equations give an excellent approximation for very long cylinders, as noted in References [9] , [10] , [11] , for which critical stress is given as [10] ;

$$\tau_{cr} = \frac{0.272\ E}{(1-\nu^2)^{3/4}} \left(\frac{t}{R}\right)^{3/2} \qquad (3)$$

Donnell, later, improved his 1933 study [9] and obtained a new set of elastic buckling equations for long and medium length cylinders. He concluded that the results obtained from these equations were in good agreement with the experimental values. Donnell also points out in Ref. [9] that the number of waves around the circumference (n) is large for short and medium length cylinders, decreasing as the length increases and taking its minimum value of two only for very long tubes. He also concludes in Ref.[9] that stability equations given in Ref.[8] will give accurate results if either the half wavelength in the circumferential or the axial direction is smaller than the radius. For the limiting case, i.e., for n=2, eqn.(2) overestimates the buckling stress higher than the actual.

The stability equations for circular cylindrical shell were also derived by Flügge [14] using a different method than Donnell's (section 2.2). His resulting equation for the critical stress of thin walled circular cylinder is identical with the equation suggested by Timoshenko [11] , and applicable to only very long cylinders.

$$\tau_{cr} = \frac{E}{3\sqrt{2}(1-\nu^2)^{3/4}} \left(\frac{t}{R}\right)^{3/2} \qquad (4)$$

It should be noted that equations (3), and (4) are applicable only to very long cylinders, boundary conditions of which are disregarded. For shorter and medium length cylinders, however, the effect of boundary conditions can no longer be ignored. The first investigation on this subject was again done by Donnell and his resulting elastic buckling equations were given above (Eqns. (1) and (2)).

In 1947, Batdorf worked on the same problem and suggested an equation given by Ref.[10] as

$$\tau_{cr} = \frac{\pi^2 D}{L^2 t} k_t \qquad (5)$$

Where D, L, and k_t are the mean diameter, length of the cylinder and a non-dimensional critical stress coefficient respectively. A graph of critical stress coefficient with respect to Batdorf Parameter ($Z = \frac{L^2}{Rt}\sqrt{1 - \nu^2}$) is also given in Ref.[10] . Equation (5) is applicable to cylinders with $Z < 10\ (R/t)^2$. For longer cylinders, i.e. $Z > 10\ (R/t)^2$, eqn.(3) rather than eqn.(5) is applicable.

The buckling stress equation of cylinders in torsion has been obtained, later, in different form by Batdorf, Stein, and Schildorout [20] . The equation is given in Ref.[12] as

$$\tau_{cr} = k_s \left[\frac{\pi^2 E}{12(1-\nu^2)(L/t)^2}\right] \qquad (6)$$

where k_s is a geometrical parameter given below. For short cylinders ($Z < 50$), end conditions are of major importance. The values of k_s are given in Ref.[12] as

$$k_s = 8.98 + 0.1Z \qquad (7)$$

if $Z<50$ (short cylinder), and

$$k_s = 0.85Z^{0.75} \tag{8}$$

if $100<Z<1.92(1-\nu^2)\left(\frac{D}{t}\right)^2$

for all end conditions Z is the Batdorf parameter as given before.

Buckling of medium length thin-walled circular cylinders was also investigated by NASA, and the following equations were reported in the monograph [15] published in 1968.

The critical buckling stress equations :

a) for long cylinders, for which $\gamma Z>78\left(\frac{R}{t}\right)^2(1-\nu^2)$

$$\tau_{cr} = \frac{\gamma E}{3\sqrt{2}(1-\nu^2)^{3/4}}\left(\frac{t}{R}\right)^{3/2} \tag{9}$$

b) for moderate length cylinders, for which

$50<\gamma Z<78\left(\frac{R}{t}\right)^2(1-\nu^2)$

$$\tau_{cr} = \frac{0.747\gamma^{3/4} E}{\left(\frac{R}{t}\right)^{5/4}\left(\frac{L}{R}\right)^{1/2}} \tag{10}$$

where Z is the Batdorf parameter and γ is the correlation factor which is given in the same reference as

$$\gamma^{3/4} = 0.67 \tag{11}$$

In the book published by Baker, Kovalevsky, and Rish [16] , on the other hand, elastic buckling stresses for thin walled circular cylinders under torsion are given as

$$\frac{\tau_{cr}}{\eta} = \frac{0.261C_s E}{(1-\nu^2)^{3/4}}\left(\frac{t}{R}\right)^{3/2} \tag{12}$$

For long cylinders, $Z>78\left(\frac{R}{t}\right)^2(1-\nu^2)$, and

$$\frac{\tau_{cr}}{\eta} = C_s \frac{Et}{RZ^{1/4}} \qquad (13)$$

for moderate length cylinders, $100>Z>78(\frac{R}{t})^2(1-\nu^2)$. In Equations (12) and (13), Z is the Batdorf parameter, η and C_s are the plasticity correction factor which is equal to unity for pure elastic buckling, and a non-dimensional coefficient given in Fig.10-11 of Ref.[16], respectively.

C.G.Foster [18] gave a summary of comparison of equations given by Ref.[16] and test results, and concluded that the equations given by Ref.[16] are not adequate in actual case.

In 1982, D.W.A.Rees [19] used modified Donnell equation for hollow cylinder with clamped ends to calculate critical plastic shear stress for buckling under torsional load, and obtained good agreement with the test results. In his calculations he used the expression

$$\tau_{cr} = \frac{0.82E_s}{(1-\nu_p)^{3/8}} (\frac{t}{R})^{5/4} (\frac{R}{L})^{1/2} \qquad (14)$$

where $\nu_p = \frac{1}{2}$, and E_s is the secant modulus at the point of buckling.

It can easily be seen that equations (3), (4), (9), and (12), which are all for long cylinders and do not contain the length as a variable, differ from each other only by modification factors. In addition, the ranges of application are also different from one another. Equations (3) and (4), for example, are applied to only infinitely long cylinders on which boundary effects are neglected as mentioned previously, whereas the term "long" is defined by boundaries for each of equations (9) and (12). Although equation (1) is also for long cylinders, it is different in form from the others, and boundary

conditions of loading for this equation are described. The elastic buckling stress equations given for moderate length thin walled circular cylinders, equations (6), (10), and (13), however, are not similar and their ranges of application are different. Rees' equation, Eqn.(14), on the other hand, is applicable to all lengths of thin walled circular cylinders with clamped ends.

The foregoing equations are tabulated in Table-1 for comparison at a glance. In the third and fourth columns, the τ_{cr} values are compared by assuming E, ν , t, R and L values.

The equations presented to determine the critical buckling stresses summarized in Table-1 are all for elastic case for which the buckling stress is below the proportional limit. But if the yielding of the cylinder occurs before buckling, the critical buckling stress will be beyond the proportional limit, i.e., on the inelastic region of the stress-strain curve of the tube material. In this case, the elastic buckling equations are not valid. Some authors [10] , [16] , modified their elastic buckling equations by simply multiplying them by a constant called PLASTICITY CORRECTION FACTOR, η . This factor is a function of the shape of the stress-strain curve, type of loading, type of the shell, and the boundary conditions. The equations given for this factor are usually given in terms of Young's modulus E, tangent modulus E_t, and secant modulus E_s which are the values at the critical buckling stress. For example, for very long cylinders, regardless of the boundary conditions and under shear loading and axial compression as well, Bleich [21] has suggested the following equation to determine the value of η ,

$$\eta = \sqrt{\frac{E_t}{E}}$$

where E_t is the tangent modulus at the point of buckling.

TABLE-1 Comparison of the Elastic Buckling Equations Using Different Values for the Material and the Geometric Parameters. ($E=10825 kg/mm^2$, $\nu=0.33$)

Ref.	EQUATIONS	L = 300 mm R = 19.0 mm t = 0.5 mm	L = 220 mm R = 20.0 mm t = 0.75 mm
[8]	$\tau_{cr}=\frac{Et^2[4.6+\sqrt{7.8+1.67(\sqrt{1-\nu^2}L^2/2Rt)^{3/2}}]}{(1-\nu^2)L^2}$	24.00	45.13
[8]	$\tau_{cr}=\frac{0.272E}{(1-\nu^2)^{3/4}}\left(\frac{t}{R}\right)^{3/2}$	13.71	23.32
[11]	$\tau_{cr}=\frac{E}{3\sqrt{2}(1-\nu^2)^{3/4}}\left(\frac{t}{R}\right)^{3/2}$	11.88	20.20
[13]	$\tau_{cr}=\frac{\pi^2 D}{L^2 t}k_t$	3.75	6.96
[20]	$\tau_{cr}=k_s\left[\frac{\pi^2 E}{12(1-\nu^2)(L/t)^2}\right]$	21.7	40.47
[15]	$\tau_{cr}=\frac{0.747\gamma^{3/4}E}{(R/t)^{5/4}(L/R)^{1/2}}$	14.45	26.96
[16]	$\tau_{cr}=\frac{0.261C_sE}{(1-\nu^2)^{3/4}}\left(\frac{t}{R}\right)^{3/2}$	8.16	13.87
[15]	$\tau_{cr}=\frac{\gamma E}{3\sqrt{2}(1-\nu^2)^{3/4}}\left(\frac{t}{R}\right)^{3/2}$	6.96	11.84
[16]	$\tau_{cr}=C_s\frac{Et}{RZ^{1/4}}$	18.16	32.88

As E_t and the critical buckling stress are interdependent, consequently, the plasticity correction factor can not be calculated without determining the buckling stress; which is also to be determined.

Some authors, [11], [12], [22], [23], on the other hand, suggested the substitution of reduced modulus E_r or tangent modulus E_t instead of Young's modulus E in elastic buckling equations to obtain plastic buckling equations for columns. This in effect is another version of the modification of E by employing the plasticity correction factor as a modification factor.

Because of the differences in the suggested buckling equations and the difficulties in the adaptation of these equations to plastic case, a new method of solution will be investigated and checked experimentally.

In this method, the buckled part of the tube is treated as a combination of curved columns of unit width and the buckling of the tube is considered as the resultant of the buckling of these columns. Plastic case will be introduced by replacing Young's modulus E in the elastic buckling equation by the tangent modulus E_t as has been previously suggested by some investigators mentioned above.

CHAPTER 3

THEORY

3.1 General

When a circular cylindrical shaft of radius R and length L is subjected to a twisting moment (torque) about its longitudinal axis (Fig.3a), the stress at any radius varies linearly with the radial distance from the axis of the cylinder as shown in Fig.3b. As the torque increases the shear stress in the outer fibers will eventually

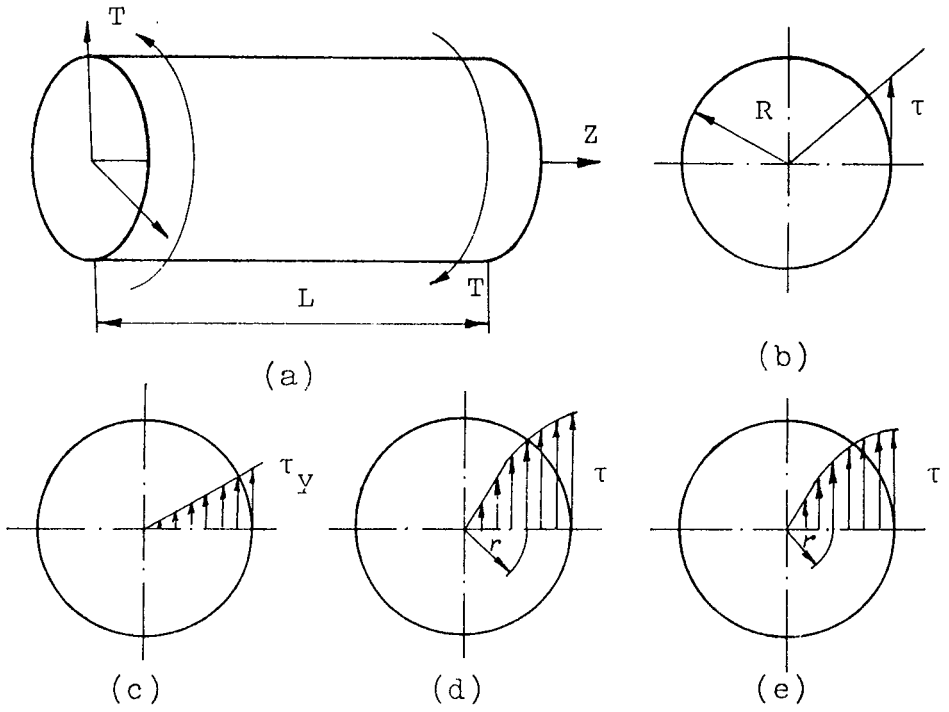

Fig.3 Stress distribution on the transverse section of a circular shaft.

reach the yield stress in shear of the material, τ_y, (Fig3c). As the torque increases further, more and more of the material will yield and the radius of the elastic core (i.e. the radius of the cylindrical surface seperating the regions of elastic and plastic strains) will decrease (Fig.3d and e). For such a situation the

stress variation would no longer be linear as in the case of elastic behaviour, but would become non linear in some fashion depending upon the shape of the shear stress-strain curve of the material. In order to obtain a solution

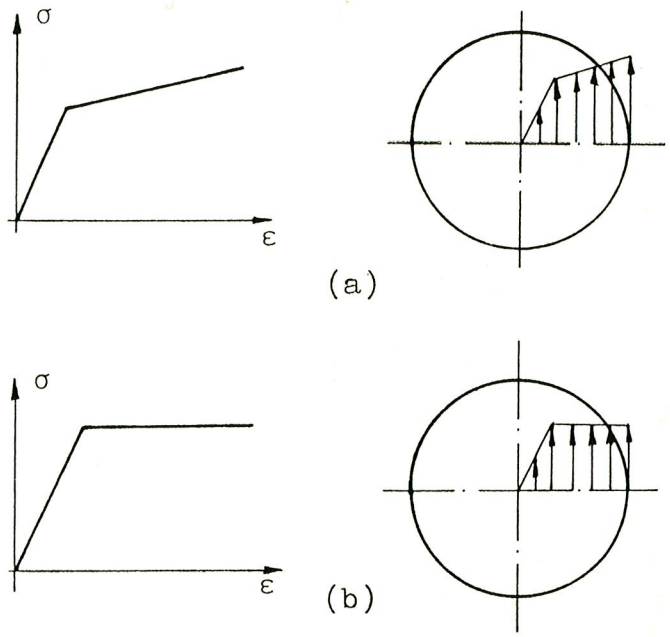

Fig.4. Idealized stress strain relations and corresponding stress distributions on the shaft cross sections;(a) elastic-linear work hardening; (b) elastic-fully plastic.

to a deformation problem, it is necessary to idealize this stress-strain relation since it may not be possible to define stress-strain curve by an equation. The stress-strain relations can be idealized as "elastic-linear work hardening" for most ductile materials (Fig.4a) or "elastic perfectly plastic at yield stress" (Fig.4b) for mild steel.

In addition to the shearing stress on transverse section, a longitudinal shearing stress τ_H is also induced which is perpendicular and numerically equal to the transverse torsional shearing stress τ_V (Fig.5a). The free body diagram of the stress element bounded by two parallel transverse planes, two longitudinal planes

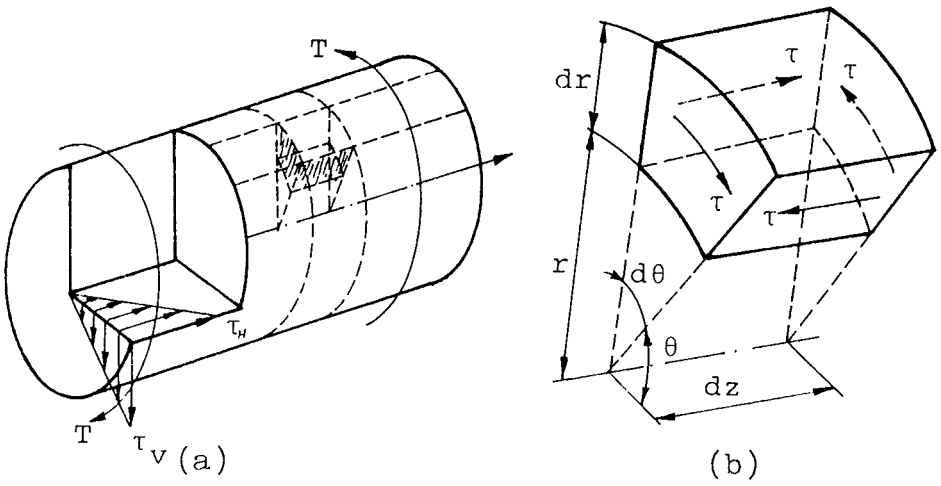

Fig.5 (a) Distribution of transverse and longitudinal shearing stress in a circular shaft under pure torsion; (b) Stresses on a stress element of the circular shaft under torsion.

through the axis, and two surfaces at different radii is shown in Fig.5b.

The stress variation on the cross-section of thin-walled circular cylinder is exactly the same as that of solid cylinder, but since most of the cross-section is removed, the outermost fibre can then be brought to yield stress with a small torque application. On the other hand, since the thickness t is small compared to the mean radius R($t/R<<1$), the variation in the stress over the thickness can be neglected.

Let us consider a homogeneous and isotropic thin walled circular cylinder of length L, wall thickness t, and undeformed mean radius R. Let r, θ , and Z denote cylindrical coordinates in radial, tangential and axial directions respectively (Fig.6a). Further, let u, v , and ω be the components of displacement of a point on the surface of the shell in the r,θ , and Z directions respectively. The free body diagram of a stress element under

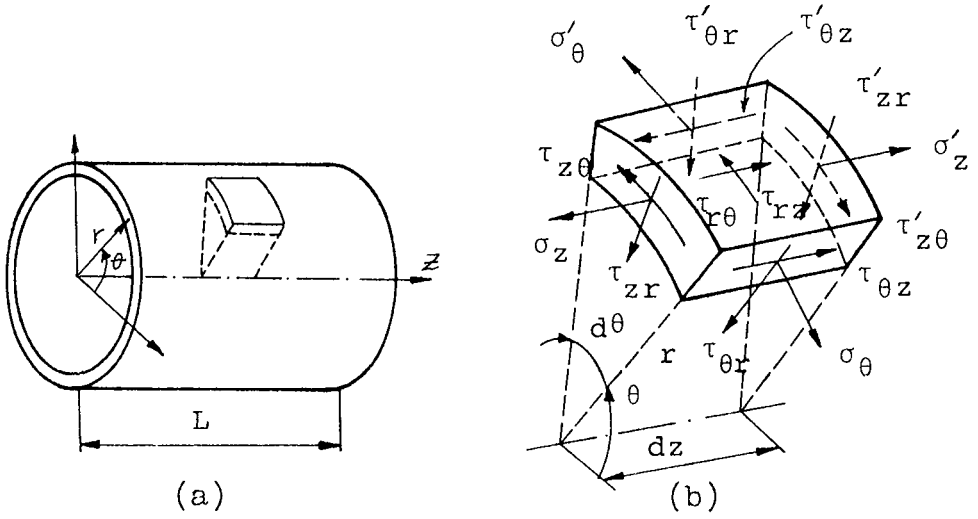

Fig.6 Free body diagram of a stress element.

general state of stresses is also shown in Fig.6b where,

$$\tau'_{\theta r} = \tau_{\theta r} + \frac{a\tau_{\theta r}}{at} d\theta \ldots (a) \qquad \tau'_{zr} = \tau_{zr} + \frac{a\tau_{zr}}{az} dz \ldots (d)$$

$$\tau'_{\theta z} = \tau_{\theta z} + \frac{a\tau_{\theta z}}{a\theta} d\theta \ldots (b) \qquad \tau'_{z\theta} = \tau_{z\theta} + \frac{a\tau_{z\theta}}{az} dz \ldots (e) \qquad (15)$$

$$\sigma'_{\theta} = \sigma_{\theta} + \frac{a\sigma_{\theta}}{a\theta} d\theta \ldots . (c) \qquad \sigma'_{z} = \sigma_{z} + \frac{a\sigma_{z}}{az} dz \ldots . (f)$$

when the cylinder is subjected to pure torsion about its longitudinal axis, in accordance with the classical theory of elasticity, most of the stress components in the stress element shown in Fig.6b vanish; the only stress components being $\tau_{\theta z}$ and $\tau_{z\theta}$ which are equal in magnitude; i.e., $\tau_{\theta z} = \tau_{z\theta} = \tau$ (Fig.5b).

From the Mohr's circle of this stress element, which is under pure shear stresses of equal magnitude (Fig.1a), it will be seen that the principal stresses, σ_1

(tensile) and σ_2 (compressive) acting on the element (Fig.1c) are equal to the shear stresses as shown in Fig.1b.

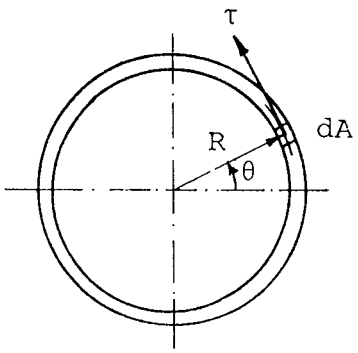

Fig.7 A thin-walled cylinder subjected to torsion.

Fig.7 shows the cross section of the thin walled circular tube. An element of force $dF_s = \tau dA$ acting on the area dA has a moment arm R to produce element of torque dT about the axis of the tube. Namely

$$dT = RdF_s = R\tau dA \tag{16}$$

integration of Eqn.16 over the area gives the total torque acting on the cross section. That is

$$T = \int R\tau dA$$

since variation in the stress over the thickness for a thin walled cylinder is neglected then τ and R are constant

$$\begin{aligned} T &= \tau R\int dA = \tau R(2\pi Rt) \\ T &= (2\pi R^2 t)\tau \end{aligned} \tag{17}$$

from which

$$\tau = \frac{T}{2\pi R^2 t} \tag{18}$$

Hence the magnitude of the principal stresses that cause buckling is

$$\sigma_1 = \sigma_2 = \sigma = \tau = \frac{T}{2\pi R^2 t} \qquad (19)$$

3.2 Column Approximation

Torsional moment T acting on the tube may be resolved into two components (Fig.8a); one perpendicular and the other parallel to surface which cuts the axis of the tube with 45°. Component T_s strains to shear the tube on 45° cutting plane whereas T_b strains to bend the tube about the major axis of the ellipse formed by 45° cutting plane (Fig.8b and c), and the compressive and tensile principal

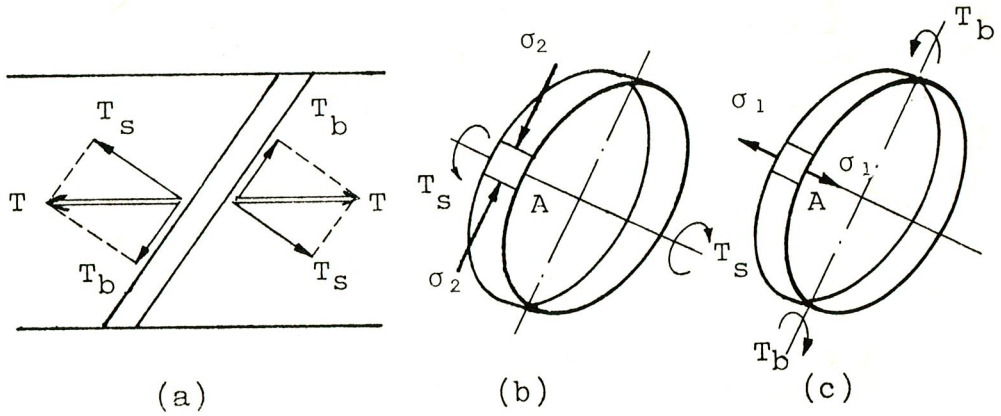

Fig.8 Resolution of torsional moment T.

stresses on the element A (Fig.1c) of the tube are created by these components respectively.

As the planes of principal stress are at 45° with the planes of maximum shearing stresses on the tube, then the buckling deformation will theoretically be along a helix which makes 45° with the axis of the cylinder. If the cylinder is cut by a plane which makes 45° with the axis, an ellipse with a minor axis b, (b = R), is obtained (Fig.9).

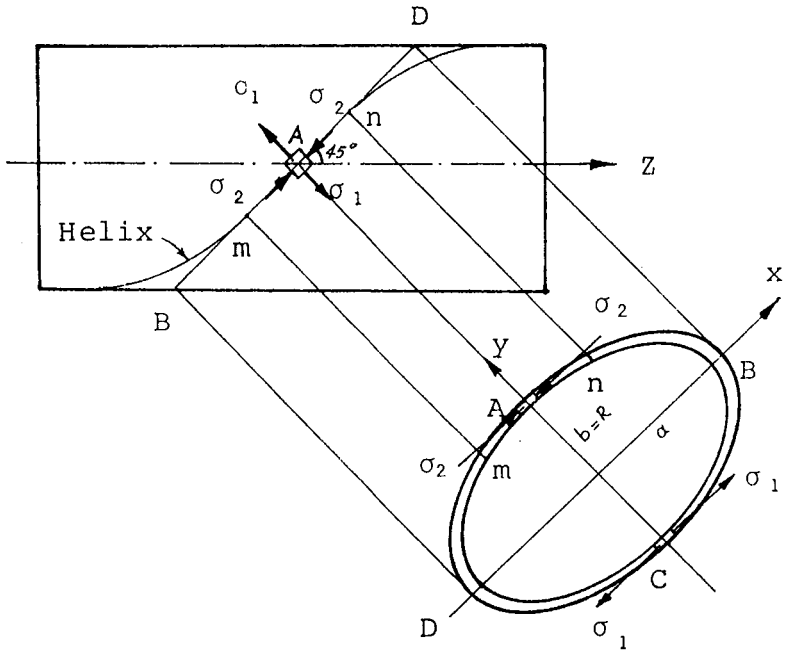

Fig.9 Stresses distribution on 45^{o} plane.

There are four important points on this ellipse; namely A, B, C, and D. Compressive σ_2 and tensile σ_1 principal stresses act on stress elements at point A and C, respectively; whereas pure shear stresses τ act on the elements at points B and D. For other stress elements between these points, the state of stress is defined by a combination of normal and shear stresses, which are smaller in magnitude than the principal stresses σ_1 and σ_2, and the maximum shearing stress τ. These states of stresses may be clearly visualized if the development of the ellipse is drawn with the development of 45^{o} helix on the same coordinate axes (Fig.10).

Since the development of the ellipse is a cosine curve(See Appendix-A for the proof), it may then be expressed for a unit minor axis (i.e., unit mean radius of the tube) as

$$h = \cos\theta \qquad (20)$$

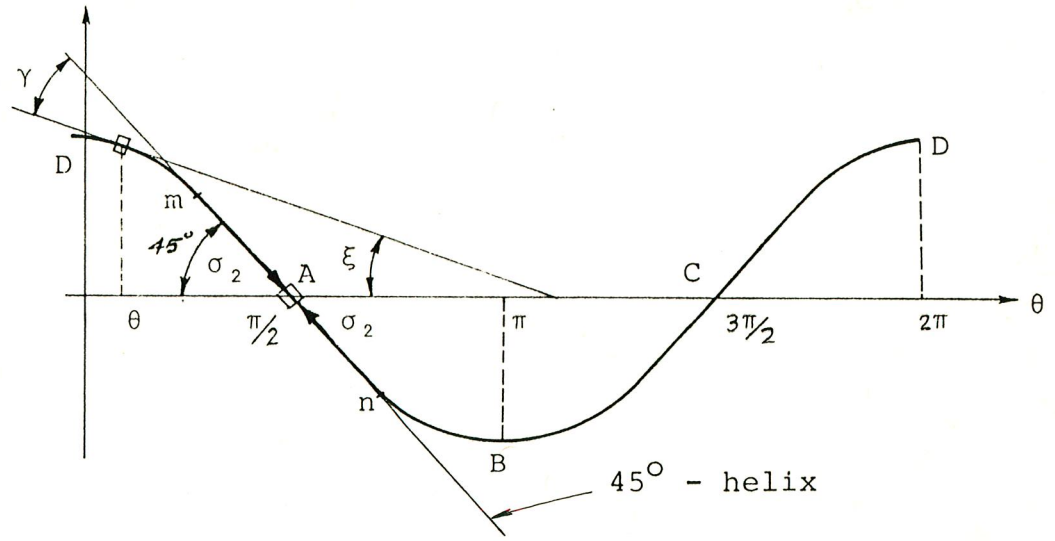

Fig.10 Development of the ellipse in Fig.9.

and the slope of this curve at any point is (Fig.10)

$$\frac{dh}{d\theta} = -\sin\theta = -\tan\xi$$

from which

$$\xi = \tan^{-1}(\sin\theta) \qquad (21)$$

the angle, γ , between the tangents of the development of the ellipse and 45° helix at any point may then be calculated from (Fig.10).

$$\gamma = 45-\xi = 45-\tan^{-1}(\sin\theta) \qquad (22)$$

A closer examination of the Fig.10 will also show that γ is also the angle between the normal stresses acting on the element of the ellipse and the principal stress directions.

Although 45° helix and 45° ellipse coincide at point A only, they may be assumed in contact along a segment m-n since the angle γ is negligibly small in

this region (about 1^{o}). Because of γ being negligibly small, the normal stresses acting on the element at this point can then be determined from Mohr's circle as

$$\sigma = \sigma_1 \cos 2\gamma = \sigma_1 \cos 2^{0} = 0.9994\ \sigma_1 \qquad (23)$$

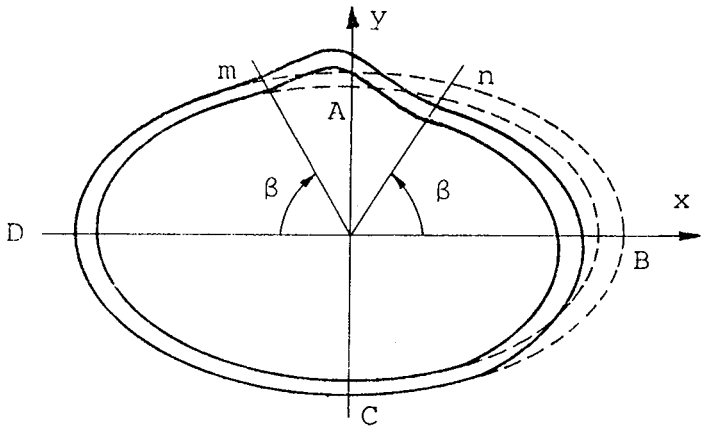

Fig.11 Cross section of a thin walled tube cut by a 45^{o} plane after torsional buckling.

The value of normal stress acting on the element of the ellipse at point n(or m) is $0.9994\ \sigma_1$ from Eqn. (23). However, it can be assumed to be equal to the principal stress without introducing appreciable error (about 0.061 percent). For $\gamma = 1^{o}$, the angle corresponding to point n on the ellipse (angle β) can be determined using the angle θ which is calculated from Eqn.(22) as

$$1^{0} = 45 - \tan^{-1}(\sin\theta)$$
$$\theta = 74.95^{0}$$

From the relationship between the angles θ and β (Appendix-A) Eqn.(14)

$$\sin^2\beta = \frac{\sin^2\theta}{1+\cos^2\theta} = \frac{\sin^2 74.95}{1+\cos^2 74.95}$$

$$\beta = 69.18^{0}$$

It is also obvious that (Fig.11) the thickness of the ellipse cut from a thin walled circular cylinder varies along the circumference. It is equal to the thickness, t, of the tube at points A and C, and $t/\sin\alpha$ for points B and D; where α is the angle of cut.
For $\alpha = 45^{o}$, this variation is about 1.03333 of the thickness at point n, which can be neglected with a maximum error of 3.333 %.

Due to the simplifying constant thickness assumption, the segment m-n could be considered to be the most critical because of the principal stresses acting along this segment.

When one considers a segment of the ellipse of length i-j, which has an infinitesimally small width, it seems reasonable to assume ends fixed; naturally this is subject to the argument that the beam should also be subjected to frictional forces on each side of the width to simulate the existing situation. Though the friction should impede the onset of buckling, it is believed that an expression developed without elaborate mathemetical variables, friction introduced as a factor, would be of more practical value.

In view of the above analysis and simplifying assumptions, it is proposed to treat the section i-j of the undeformed ellipse as a curved bar with fixed ends (Fig.12) for which the effective length l_e is m-n. The Euler equation for the columns having other than hinged ends is [24]

$$P_{cr} = \frac{\pi^2 EI}{(Kl)^2} \qquad (24)$$

where E is the modulus of elasticity, I the second moment of area of column cross section, and (Kl) is the length between inflection points and is known as "Effective Length".

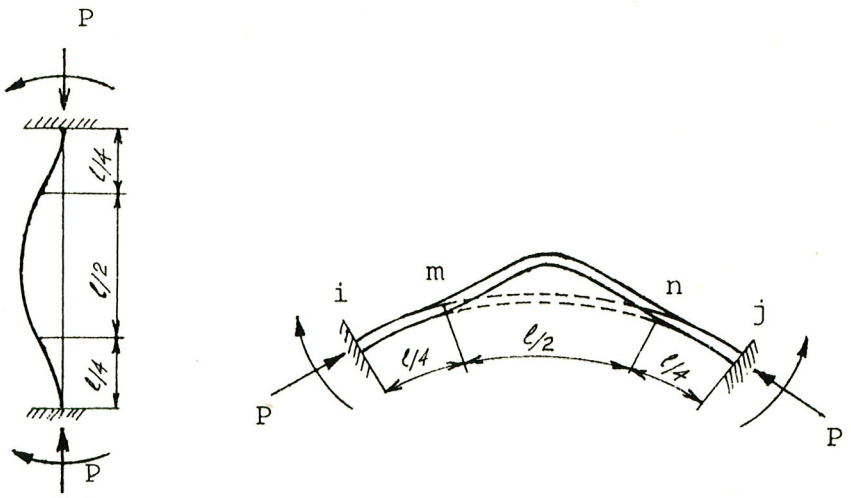

Fig.12 Buckling of a uniform elastic column with fixed ends; (a) straight; (b) curved

Substituting $Kl = l_e$, $I = \frac{bt^3}{12}$, and $P_{cr} = \sigma_{cr} b t$ into Eqn.(24) and simplifying,

$$\sigma_{cr} = \frac{\pi^2 E t^2}{12 l_e^2} \tag{25}$$

It is common knowledge that the elastic buckling phenomenon depends upon the h/l ratio where l is the length and h the thickness of the column symbolized as t for the thin walled torsional cylinder. For elastic buckling to prevail, this ratio must be very small, i.e., $h/l << 1$. For short columns, however, the buckling phenomenon will not occur until the compressive stresses exceed the proportional limit of the material. Consequently the buckling load must be determined by taking inelastic column behaviour into account. Drawing a parallel between the buckling phenomenon in the elastic and the plastic region, it has been suggested by Engesser [25] to employ Eqn.(24)in the plastic region simply by substituting the tangent modulus E_t under increasing loading or double modulus $\bar{E}$ under constant loading for Young's modulus E in the said equation.

For a given mean radius R of the tube, the length of the segment m-n is constant (Figs.9, 11). The type of column action will then depend upon the thickness of this segment. When the thickness is small, elastic buckling preceeds plastic buckling or vice versa. So, the thickness-to-radius ratio (t/R) is an important parameter for the type of buckling failure of thin walled circular cylinders under torsional loading.

When a column is subjected to a uniaxial compressive load, a stress element in the column is subjected to uniaxial compressive stresses σ and the strains are

$$\varepsilon_x = -\frac{\sigma}{E}, \quad \varepsilon_y = \nu\varepsilon_x, \quad \varepsilon_z = \nu\varepsilon_x \tag{26}$$

Provided that there is no column action, the expressions signify an elastic deformation (Fig.13a). However if a particular case of biaxial loading is considered (Fig.13b), the buckling failure can no longer be predicted by Eqn. (25). Buckling will be favored or hindered depending upon the algebraic sign of the principal stresses.

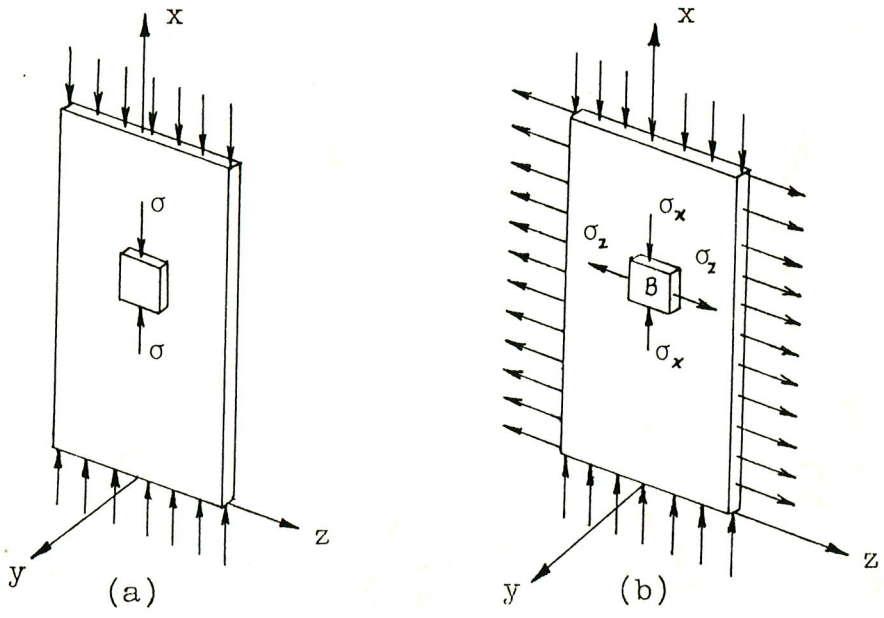

Fig.13 State of stresses in column under different loadings, (a)uniaxial loading; (b) biaxial loading.

Let us take a column element B under biaxial stresses (Fig.13b); which is the same condition for the stress element at point A of Fig.9. Let the strip in Fig.13b represent a portion of the segment i-j. The strains along the three mutually perpendicular axes of the stress element will be

$$\varepsilon_x = \frac{1}{E}[\sigma_x - \nu(\sigma_y + \sigma_z)] \quad \ldots\ (a)$$

$$\varepsilon_y = \frac{1}{E}[\sigma_y - \nu(\sigma_x + \sigma_z)] \quad \ldots\ (b) \qquad (27)$$

$$\varepsilon_z = \frac{1}{E}[\sigma_z - \nu(\sigma_x + \sigma_y)] \quad \ldots\ (c)$$

since σ_x is negative and $\sigma_y = 0$ (Fig.13b), then Eqn. (27a) becomes

$$\sigma_x = \frac{1}{E}\ [-\sigma_x - \nu\sigma_z\ ] \qquad (28)$$

From Fig.9, $\sigma_x = \sigma_z$, Eqn.(28) reduces to

$$\varepsilon_x = -\frac{\sigma_x}{E}(1+\nu) \qquad (29)$$

since the strain for buckling is fixed for a given column, then equating the Eqns. (26) and (29),

$$-\frac{\sigma}{E} = -\frac{\sigma_x}{E}(1+\nu)$$

or

$$\sigma_x = \frac{\sigma}{1+\nu} \qquad (30)$$

Substituting $\tau_b = \sigma_x$ and $\sigma = \sigma_{cr}$ in Eqn.(30) at the onset of buckling

$$\tau_b = \frac{\sigma_{cr}}{1+\nu} \qquad (31)$$

Thus the critical stress for buckling of a column

under biaxial stresses can be calculated by substituting Eqn.(25) into Eqn.(31)

$$\tau_b = \frac{1}{1+\nu} \frac{\pi^2 E t^2}{12(l_e)^2} \tag{32}$$

since E is replaced by E_t and $\nu = 0.5$ for plastic deformation, Eqn.(32) then becomes

$$\tau_b = \frac{\pi^2 E_t t^2}{18(l_e)^2} \tag{32a}$$

Equation(32a) is the proposed expression to predict the plastic torsional buckling of thin-walled circular cylinders.

In order to employ Eqn.(32a), tangent modulus E_t and the effective column length l_e must be determined since t is known. In determining these values a method similar to those in Refs. [23] , and [24] given for elastic buckling (E=constant) will be followed; although a trial and error procedure is suggested for inelastic buckling of a column of known dimensions in the same references.

When buckling phenomenon is concerned, it is well known that the critical buckling stress is related to the length of the column. Consequently, the length l is also related to the tangent modulus E_t at this critical stress. For example, for the same thickness of the column, as the length decreases the buckling stress will increase and hence the corresponding tangent modulus will decrease as shown in Fig.14a. The relation between l and E_t must then be determined to calculate the critical buckling stress.

If the true stress versus tangent modulus ($\bar{\sigma}$-E_t) curve Fig.14b is drawn by using true stress-true strain curve, tangent modulus at any stress value can be obtained. Since l is constant for a given tube of mean radius R, using the proposed equation for buckling, Eqn.(32 a) and $\bar{\sigma}$-E_t curve, tangent modulus versus radius-to-thickness

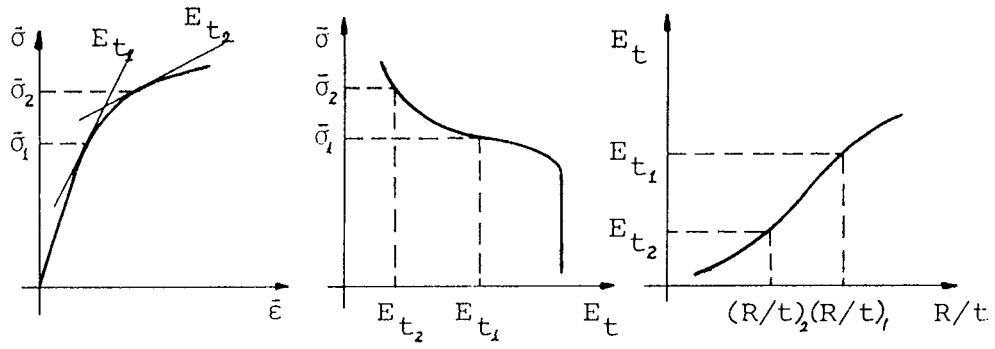

Fig.14 (a) Stress-strain curve
(b) Stress-tangent modulus curve
(c) Tangent modulus - R/t ratio curve

ratio (E_t - R/t) curve can be drawn (Fig.14c), which gives the relation between E_t and R/t.

There is no method to determine the critical length, (m-n), in the relevant literature. The following method based on some analytical considerations is suggested as a first approximation to the solution of the problem. The validity of this approach is going to be checked during the experimental work. Should the result be negative, an attempt will be made to determine the critical length empirically.

Arc length of the development of the ellipse can be calculated using Eqn.(20) from

$$S = \int_0^{\pi/2} \sqrt{1+(dh/d\theta)^2}\, d\theta \qquad (33)$$

as

$$S = \int_0^{\pi/2} \sqrt{1+\sin^2\theta}\, d\theta \qquad (34)$$

Eqn.(34) has no analytical solution. Then cosine curve of the development of the ellipse must be approximated

by a curve for which Eqn.(33) has an analytical solution. A parabola, the equation of which is

$$h = -\frac{4}{\pi^2}\left(\theta^2 - \frac{\pi^2}{4}\right) \tag{35}$$

can be used instead of Eqn.(20) in the calculation of arc length with an error of 0.149 % (See Appendix-B) for the interval $0 \leq \theta \leq \frac{\pi}{2}$. From Eqn.(20) of Appendix-B,

$$S = \frac{\pi^2}{8}\left[\frac{u\sqrt{1+u^2}}{2} + \frac{1}{2}\ln\left(u+\sqrt{1+u^2}\right)\right]$$

where $u = \frac{8\theta}{\pi^2}$, θ is in radian. Substituting 74.95° = 1.308 rad. for θ , arc length B-m can be calculated as

$$S_{Bn} = 1.52289$$

It is well worth reminding that Eqn.(20) and the following equations to approximate the peripherial length of the ellipse were based on a radius of unity. The actual arc length of a tube of a given diameter is therefore the product of the above expression with the corresponding radius.

$$S_{Bn} = 1.52289\ R \tag{36}$$

Peripherial length of an ellipse can be calculated from

$$P = 2\pi\sqrt{\frac{1}{2}\left(a^2 + b^2\right)} \tag{37}$$

where a and b are the major and minor axes of the ellipse respectively. Substitution of b = R and a=R/sin45 into Eqn.(37) results

$$P = 7.6953\ R \tag{38}$$

From Figs.10 and 11, $S_{An}=S_{AB}-S_{Bn}$, $S_{AB} = P/4$, and $S_{mn} = 2S_{An}$, then the length of the segment m-n is

$$S_{mn} = 0.802\,R \tag{39}$$

Hence, substituting $l_e = S_{mn} = 0.802R$ into Eqn.(33) yields

$$\tau_b = \frac{\pi^2 E_t}{15.4369\ (R/t)^2} \tag{40}$$

Eqn.(40) can be used to estimate the critical buckling stress when R/t ratio is calculated and E_t is determined from the R/t - E_t curve as was described and illustrated in the Fig.14. But since E_t and R/t values are obtained from the equivalent stress-equivalent strain curve, which is formed as the true stress-true strain diagram for pure tension, then the critical buckling stress calculated from Eqn.(40) will be the equivalent stress for buckling.

For an isotropic strain-hardening material, Von Mises yield criterion for the general state of stresses on the stress element of the ellipse cut from the tube (Fig.15) is,

$$2\bar{\sigma}^2 = (\sigma_\rho - \sigma_{\beta'})^2 + (\sigma_{\beta'} - \sigma_{z'})^2 + (\sigma_{z'} - \sigma_\rho)^2 + 6\,(\tau^2_{\rho\beta'} + \tau^2_{\beta'z'} + \tau^2_{z'\rho}) \tag{41}$$

where $\bar{\sigma}$ is the equivalent stress and subscripts ρ, β', and z' denote the directions of the stresses on the elliptical cross section of the tube cut by a 45° plane (see Fig.15)

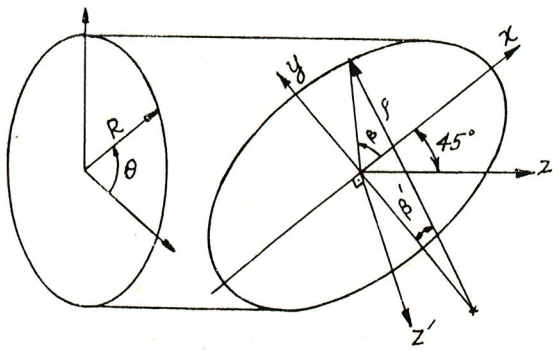

Fig.15 Coordinate axes on transverse and 45° planes of a circular cylinder.

Assuming the stress-strain curves of the tube material for tension and compression to be identical, all of the terms on the right-hand side of Eqn.(41) will vanish except $\sigma_{\beta'}$ for pure compression since the element on the ellipse is under compressive stresses. Then Eqn.(41) becomes

$$\bar{\sigma} = \sigma_{\beta'} \tag{42}$$

On the other hand, Eqn.(41) reduces to

$$\tau_{\theta z} = \frac{1}{\sqrt{3}} \bar{\sigma} \tag{43}$$

if Eqn.(41) is written for stress element on the tube using the coordinate axes, r, θ, and Z and applied for pure torsional loading for which $\sigma_r = \sigma_\theta = \sigma_z = \tau_{r\theta} = \tau_{zr} = 0$ but $\tau_{\theta z} \neq 0$. From Eqns (42) and (43).

$$\tau_{\theta z} = \frac{1}{\sqrt{3}} \sigma_{\beta'} \tag{44}$$

Hence in order to compare the theoretical stress calculated by the proposed equation (Eqn.(40)) with the experimental value calculated by Eqn.(19), Eqn.(19) should be multiplied by $\sqrt{3}$ or vice versa. Then the pure shear stress for buckling of the thin walled circular cylinders is

$$\tau_{\theta z} = \tau = \frac{1}{\sqrt{3}} \frac{\pi^2 E_t}{15.4369 (R/t)^2} \tag{45}$$

or

$$\tau = \frac{0.36913\ E_t}{(R/t)^2} \tag{46}$$

On the other hand, as was stated previously, the transverse edges of the assumed column i-j are not free, but resisted by the adjacent columns' surfaces as illustrated in Fig.16. Thus the column action of a critical strip is also resisted by the elements on each side, which will increase the buckling strength. This increase is compensated by the decrease of buckling stress due to the modification of Euler equation for biaxial loading case.

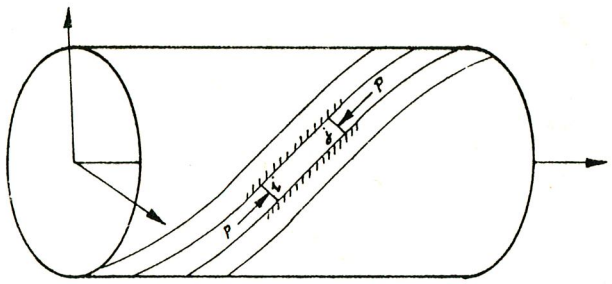

Fig.16 Transverse edges of the assumed column on the cylinder are resisted by the adjacent columns.

Equation (46) is the proposed equation for the buckling of a thin walled circular cylinder and can be evaluated when (R/t) is calculated and E_t is determined from the (R/t - E_t) curve as was described and illustrated in the Fig.14.

The experimental evaluation of the plastic buckling stresses is going to be treated in the following chapter.

CHAPTER 4

EXPERIMENTAL RESULTS

The method of analysis presented in Chapter-3 was evaluated by conducting

i- torsion test to determine the onset of buckling.

ii-tension test to obtain the mechanical properties of the materials used in the experiments.

4.1 Torsion Test

Application of twisting load to a thin-walled cylindrical specimen presents special problems. These are :

a- Uniform application of the twisting torque along the circumference,

b- Gripping the specimen without crushing the ends of the tube, which alters the end conditions.

An apparatus was designed and constructed to affect this end. A torsiometer was also in corporated in the apparatus to measure the angle of twist of the specimen (Fig.17).

Crushing of the ends was prevented by inserting plugs from both ends with slight interference. In order to assure that there was no slippage during the experiments, the plugs were knurled to bite slightly into the specimen.

Uniform biting was affected by employing two halved grips at the ends. The grips were first bored to the outer diameter of the specimen then parted symmetrically. The two halves were lightly machined to provide sufficient clearance for the squeezing action upon tightening of the allen screws.

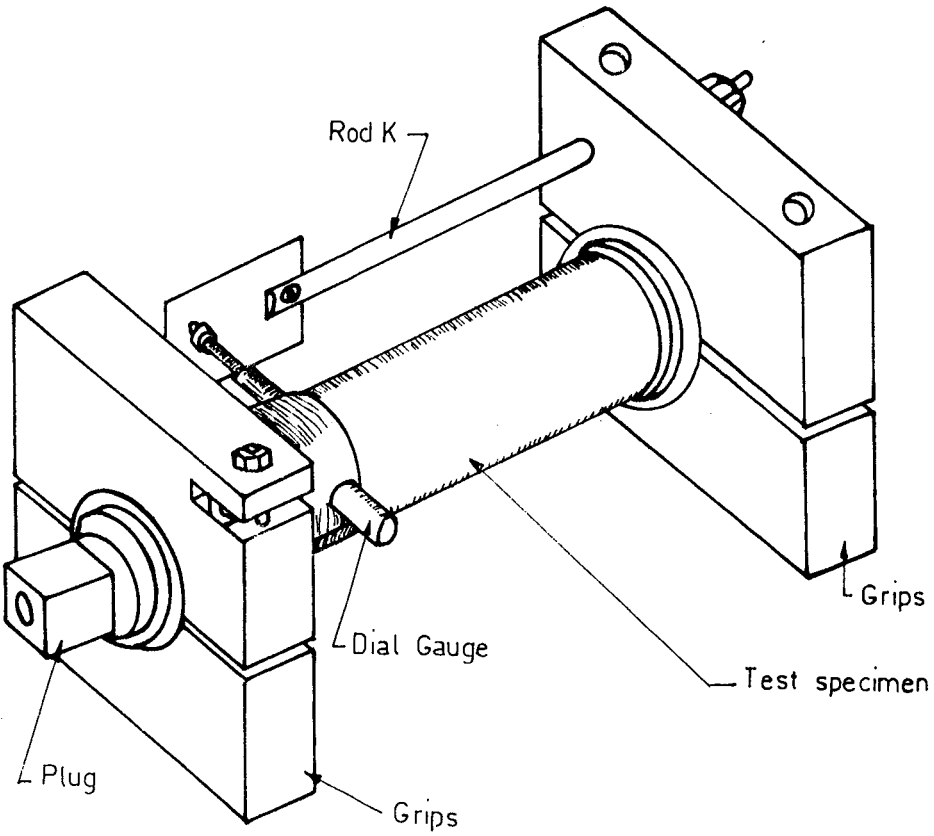

Fig.17 Test specimen with the gripping apparatus and the torsiometer.

The ends of the plugs were machined to obtain a rectangular prism with a square base. This was needed to employ the four-jaw universal chucks on the torsion tester. Besides uniform gripping, this arrangement ensured that the weights of the grips were totally taken by plugs; thus avoiding anomalous bending effects creeping into the experiments. It can be said that the tubular specimens were subjected to pure torsion alone.

Furthermore, a torsiometer was also incorporated in the apparatus to measure the angle of twist of the specimen. A dial gauge system was mounted on this apparatus with which the angle of twist was accurately

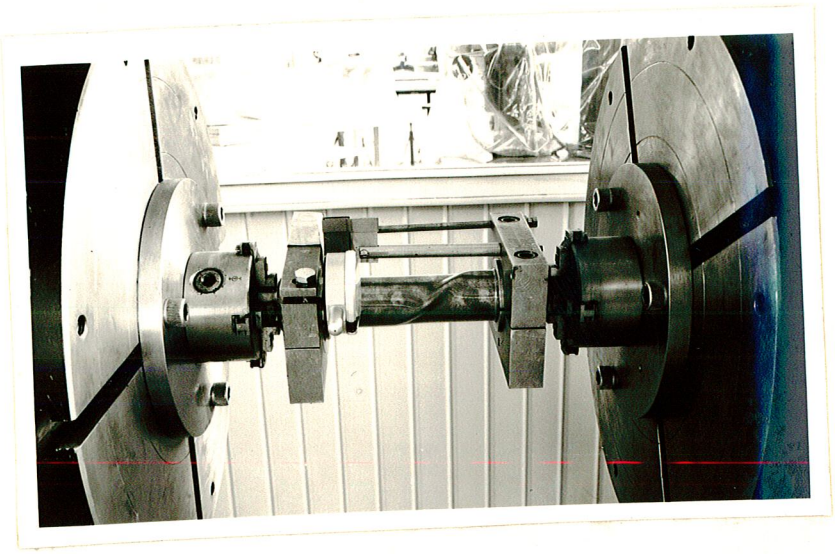

Fig.18 A photograph showing the plastic buckling failure of a torsion specimen.

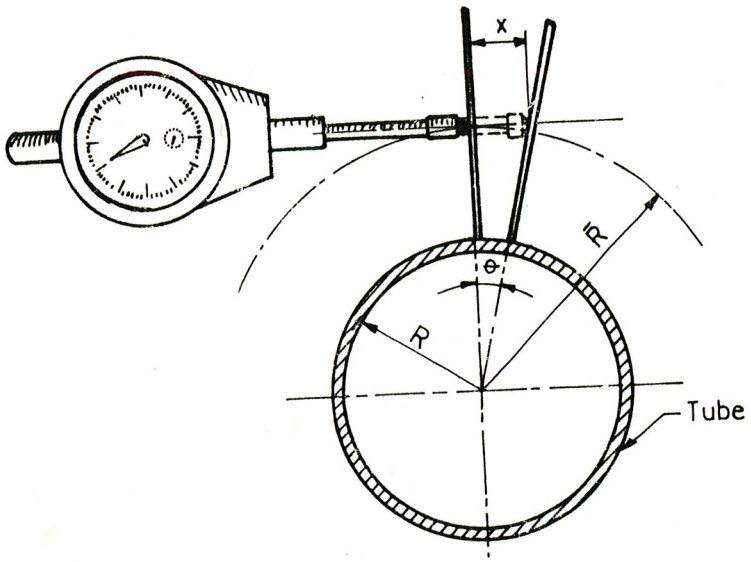

Fig.19 Determining the angle of twist.

measured in addition to the values taken from the scale on the straining head of the testing machine.

This system consisted of two parts; a dial gauge and a rod (Figs.17, 18). The dial gauge was fitted to the grip at the sensing head of the machine. The cantilever rod (rod K in Fig.17) was fitted firmly to the grip on the rotating end of the specimen; ensuring its parallelism to the axis of the tube. The plunger of the dial gauge rested on a flat plate attached to the end of the rod. It can be followed from Fig.19 that the angle of twist, θ , is the arctangent of $x/\overline{R}$.

The configuration that was given to the torsion specimens is shown in Fig.20 and the dimensions are given in Table-2. These dimensions were decided based on the following considerations :

1- Dimensions of the available tubes,

2- Problems involving machining, and

3- To ensure plastic buckling which is dictated by the thickness-to-radius ratio, (t/R).

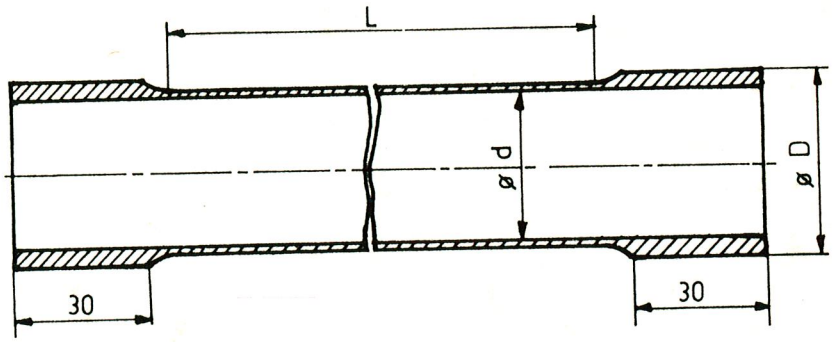

All dimensions are in mm

Fig.20 Torsion Test Specimen

TABLE-2 Dimensions of the torsion specimens (in mm)

Specimen		L	D	d	R	t	R/t
COPPER	A_1	200	39.54	37.32	19.315	0.91	21.23
	A_2	200	39.44	37.66	19.275	0.89	21.66
	A_3	120	39.30	37.36	19.165	0.97	19.76
	A_4	120	39.15	37.30	19.1125	0.925	20.66
	B_1	220	38.85	36.00	18.7125	1.425	13.132
	B_2	220	39.00	36.30	18.825	1.35	13.944
	B_3	220	39.00	36.2	18.80	1.40	13.43
	C_1	200	39.28	37.80	19.27	0.74	26.04
	C_2	120	39.30	37.40	19.175	0.95	20.185
BRASS	D_1	120	34.65	33.14	19.9475	0.755	22.45
	D_2	120	34.72	33.19	16.9775	0.765	22.20
	D_3	120	34.80	33.24	17.01	0.78	21.81
	D_4	120	34.65	33.16	16.9525	0.745	22.76

The specimens prepared from cold drawn tubes were annealed to relieve the internal stresses and to increase their ductility.

To ensure the concentricity of the inner and outer surfaces of the tube and to minimize the variations in thickness, the tubes were machined inside and outside. At first, the specimens were cut-off in the required length and their internal surfaces were machined until complete cylindricity was obtained. Later, using the bore as a baseline, outside of the tubes were machined by fitting the tube over a mandrel.

Plugs were inserted into the specimen at both ends. The rod shown in Fig.21 was used to align the plugs during this operation. The grips were then introduced using the special jig shown in Fig.22 to ensure the parallelism of the grips. The assembly, consisting of grips, plugs and torsiometer, was chucked to the torsion tester and tested until buckling proceeded.

The testing machine used in the experiments was 4000 Nm capacity TREBEL Torsion Tester (Fig.23). This machine is equipped with an electronic sensing head in which the torque acting on the test specimen is converted into an electrical signal and indicated by a dial on the control unit (Fig.23).

The machine is capable of applying torques 1/10, 1/5, 1/2, and 1/1 of the full capacity which facilitated the choice of the scale compatible with the dimensions of the specimens. The tester is also equipped with an angular displacement transducer to measure the angle of twist. Both the applied torque and the angle of twist can be plotted with an x-y recorder to obtain the torque-twist diagram (Fig.24).

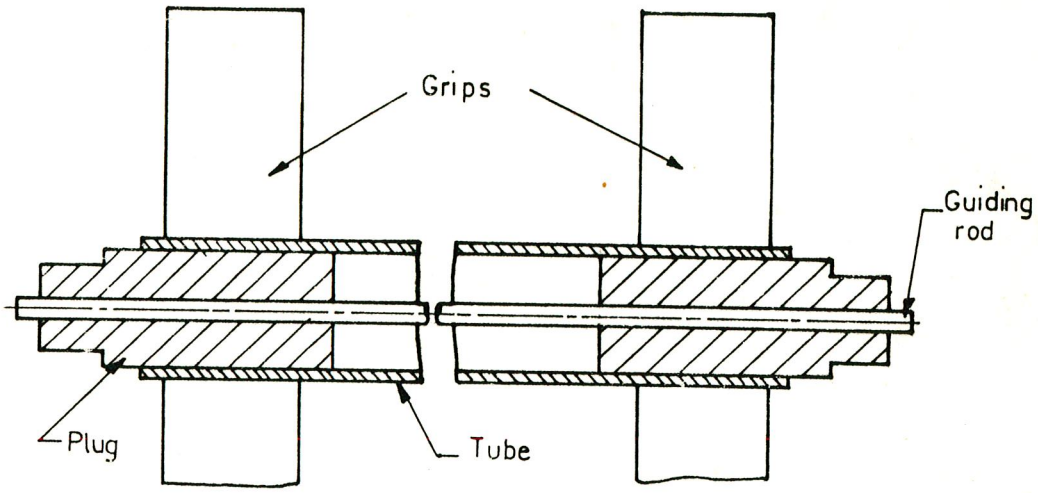

Fig.21 Alignment of plugs

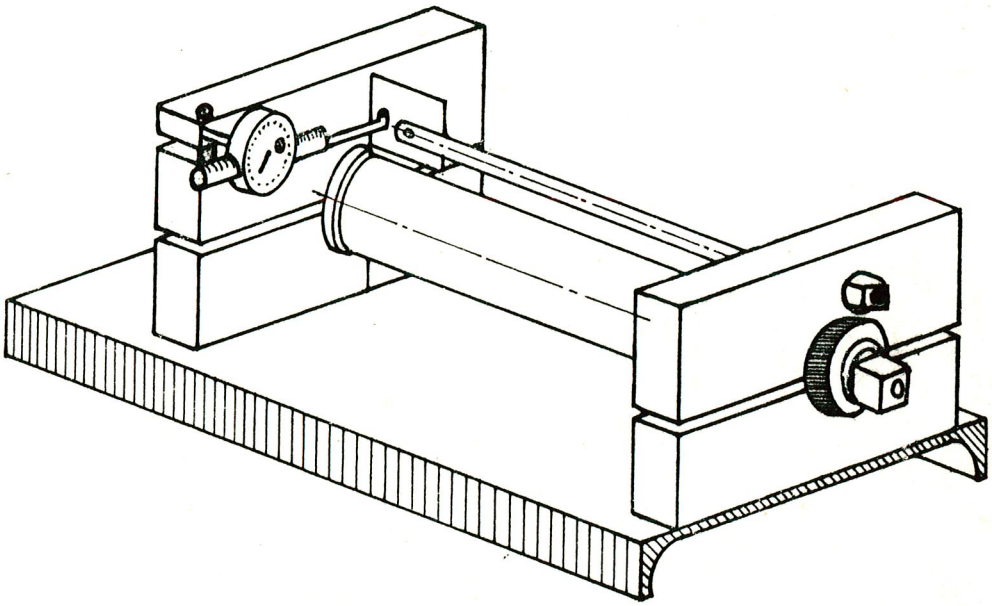

Fig.22 Mounting jig for torsion specimens

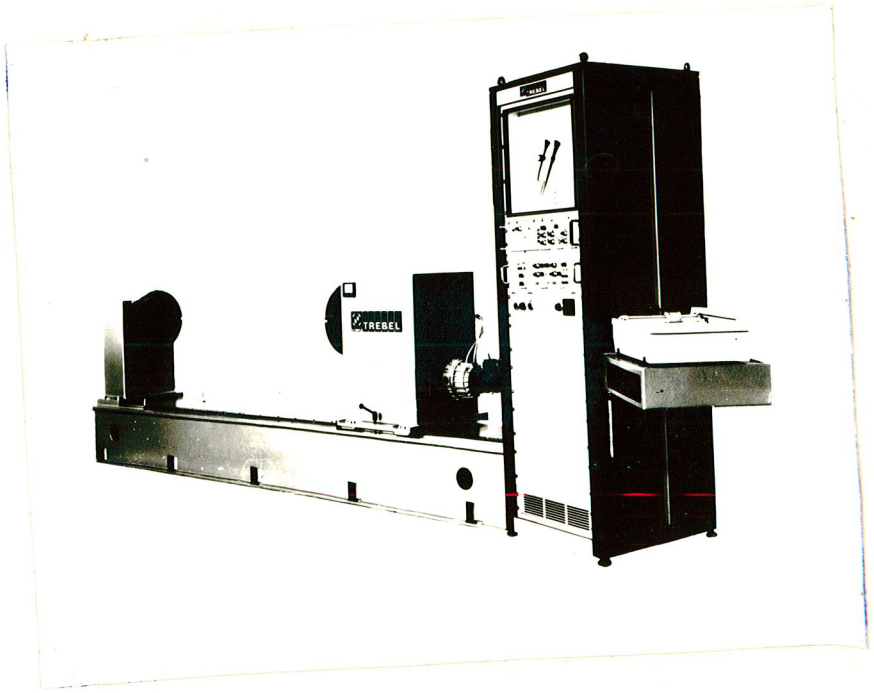

Fig.23 Torsion Testing Machine

After mounting the described assembly in the machine, torsional load was applied at a rate comparable to that of a tension test. Torque was applied until the buckling proceeded; which was indicated by a continuous decrease in the torque required to twist the specimen. Fig.18 shows a typical buckling failure of the specimen.

The testing was stopped upon buckling of the specimen and the reading on the torsiometer, the angular rotation of the loading head, and the torque were recorded. The angle of twist given by the torsiometer was used to convert the plotted torque twist diagram to the actual torque twist diagram of the specimen. A close examination of Fig.18 will indicate the necessity of this step. As the torsion tester measures the angular displacement of the straining head, the angle of twist measured by the tester is then indicated by the distance between the two face

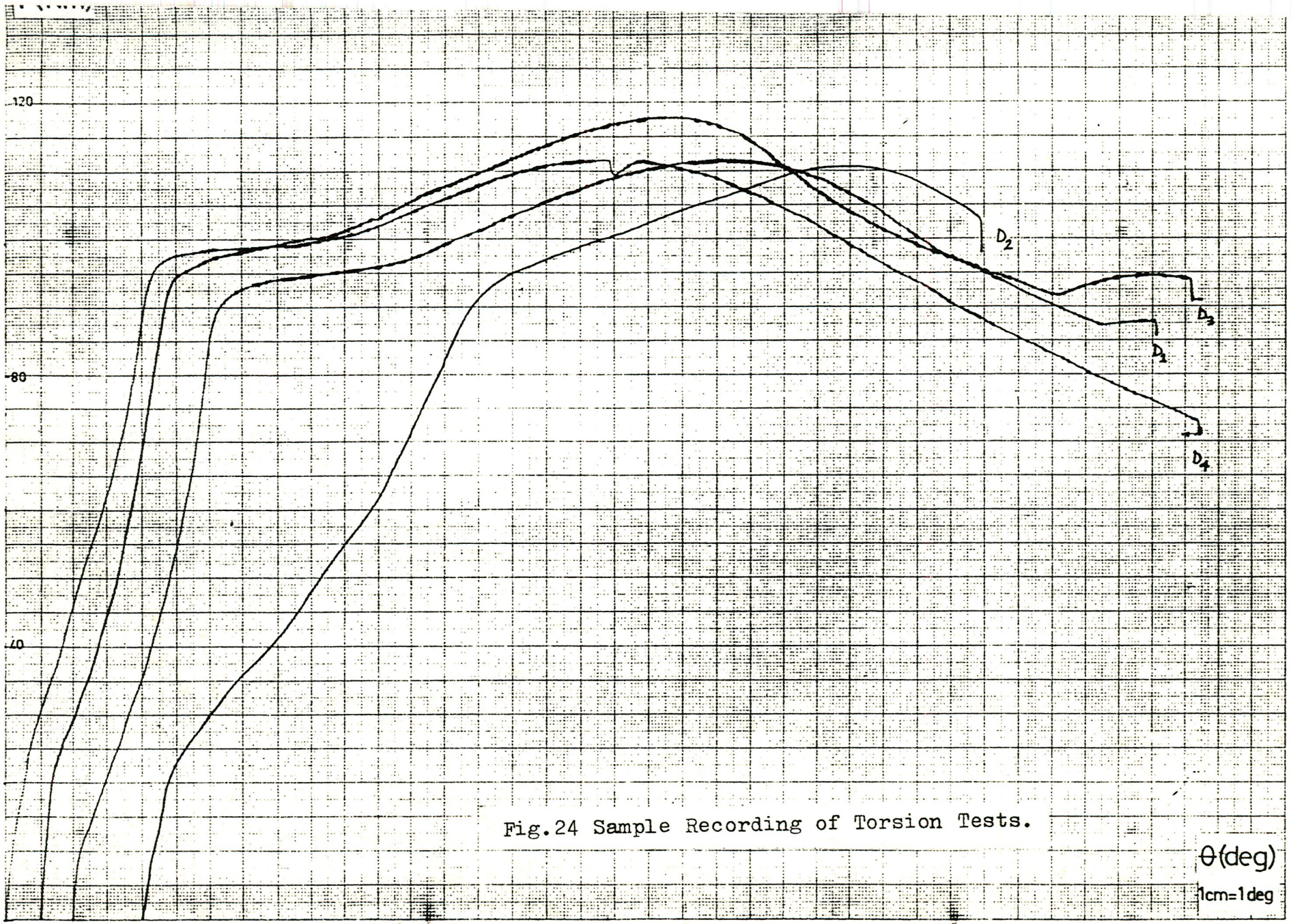

Fig.24 Sample Recording of Torsion Tests.

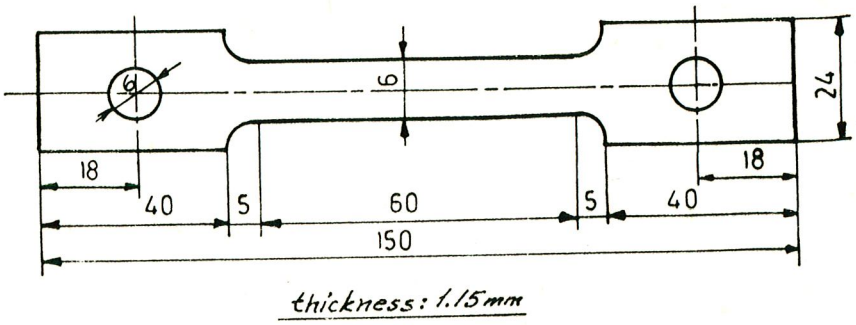

Fig.25 Tension Test Specimen

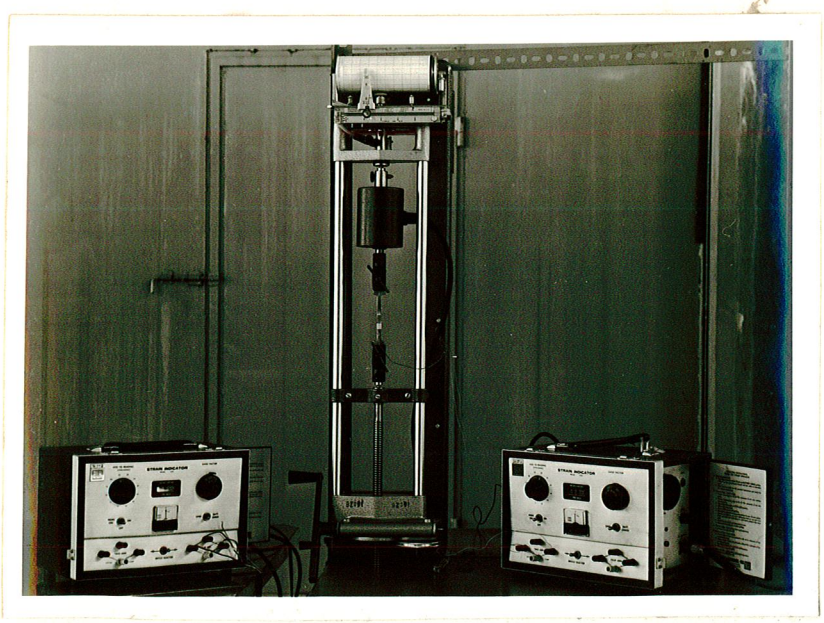

Fig.26 Tension Test Rig

plates. Considering the geometric similarity, the actual angle of twist of the specimen is proportional to the plotted θ value by an amount indicated by the torsiometer.

Three sets of copper and one set of brass specimens were used in these experiments. They were selected because of their ductility; which facilitated the demonstration of the plastic behaviour. Brass and copper specimens were prepared from brass and copper tubes manufactured by RABAK designated as DIN 17671 and DIN 40500 respectively. The other set of copper specimens were prepared from the tubes manufactured by MKE. Each set of specimens were annealed at different temperatures, to obtain specimens of different mechanical properties.

The results obtained from copper and brass specimens are presented in Table-3.

4.2 Tension Test

In Eqn.(46), which was proposed to predict the onset of buckling, tangent modulus E_t is another variable which must be determined experimentally from tension test.

Tensile test specimens (See Figs.25 and 26, Fig. D2 of Appendix-D) were prepared from the tubes used in torsion tests and pulled in the MONSANTO Tensometer (Bench Type Tensile Tester), (Fig.26). The full details of this tester is appended to the thesis.

The tensile test results were later converted to the true stress-true strain ($\bar{\sigma}$-$\bar{\varepsilon}$) diagrams. The $\bar{\sigma}$-$\bar{\varepsilon}$ diagrams of the materials used in the torsion tests are presented in Figs.(27).

In the evaluation of Eqn.(46), tangent modulus E_t versus radius-to-thickness ratio graph is required as was mentioned in Chapter-3. To determine the tangent modulus

TABLE-3 Theoretical and Experimental Critical Buckling Stresses of Thin-Walled Circular Tubes Under Torsion.

Specimen		τ Experimental (Kg/mm^2)	τ Theoretical (Kg/mm^2)	% error
COPPER	A_1	5.1627	5.162	- 0.077
	A_2	5.051	5.121	+ 1.4
	A_3	5.512	5.295	- 3.93
	A_4	5.164	5.212	+ 0.94
	B_1	10.782	11.017	+ 2.18
	B_2	10.685	10.947	+ 2.45
	B_3	10.823	10.999	+ 1.63
	C_1	6.083	6.133	+ 0.41
	C_2	6.737	6.886	+ 2.21
BRASS	D_1	8.344	8.010	- 4.01
	D_2	8.280	8.014	- 3.21
	D_3	8.450	8.150	- 3.54
	D_4	8.338	7.937	- 4.81

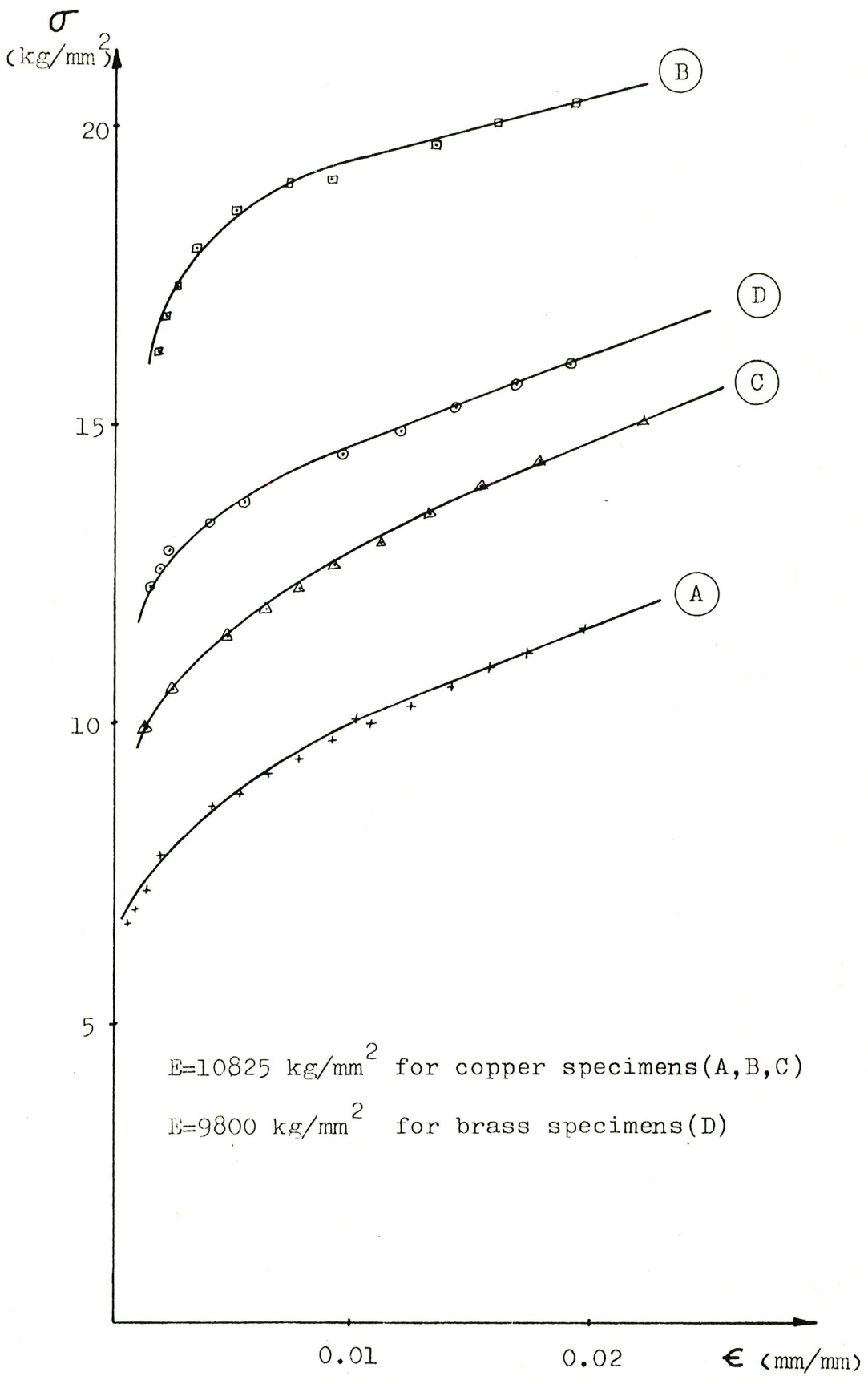

Fig. 27 True stress-True strain diagrams of the tube materials used in the experiments.

at any stress value, at first, the true strain-true strain curves of the tube materials were obtained by employing Swift's expression

$$\bar{\sigma} = A(B + \bar{\varepsilon})^{n} \qquad (47)$$

where A, B and n are constants for a given material. These constants were determined by the method suggested by Sıvacı and Kaftanoğlu [26] . Since the tangent modulus is the slope of the stress-strain curve defined by Eqn. (47), it can be defined as

$$E_t = \frac{d\bar{\sigma}}{d\bar{\varepsilon}} = nA(B + \bar{\varepsilon})^{n-1} \qquad (48)$$

A computer program was written for the calculation of constants of Eqn.(47);which is given in Appendix-E. The values computed for these constants are tabulated in Table-4.

Another popular expression for the plastic behaviour is put forward by Ludwik. The plastic behaviours of the materials used in the experiments were also determined according to the Ludwik's expression. In comparison, Swift's expression was seen to approximate the actual behaviour more closely.

4.3 Evaluation of Results

The torsional load required to cause the plastic buckling of specimens as predicted by Eqn.(46) and the actual experimental results were tabulated in Table-3.

As can be seen from Table-3, all of the theoretical results are closely in agreement with the experimental results. Besides the numerical, the experimental results have also verified that some of the assumptions made were also physically feasible.

An examination of the Fig.(28),which shows a cut away view of the deformed specimen, indicates that

TABLE-4 Constants of Swift's Expression for the materials used in the experiments.

Materials	Constants		
	A	B	n
Copper-A	27.5	0.00172	0.2441
Copper-B	387.5	0.19978	1.9576
Copper-C	38.6	0.00308	0.25254
Brass-D	52.5	0.01307	0.34169

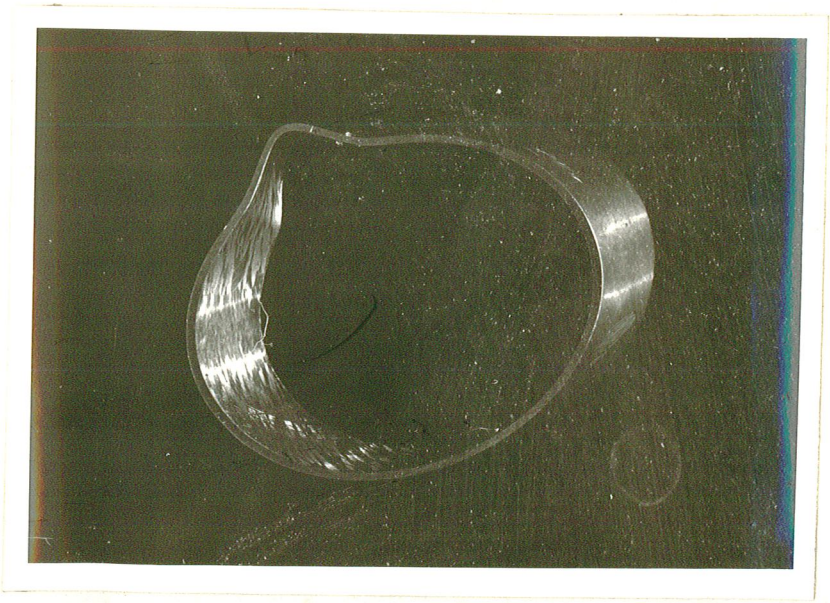

Fig.28 Cut-away view of the deformed specimen.

plastic buckling due to twisting is highly localized at a point on this 45^{o} plane; as is indicated by heavy bulging. A further examination of the deformed specimen shows that this point is coincident with the point A in Figs.(10) and (11) of the theoretical analysis;which is a proof of the assumption that the onset of buckling starts from the thinnest section on the ellipse.

Though the theoretical results are closely in agreement with the experimental results, slight differences between the two merit a further discussion.

The deviations between the theoretical and experimental results stem from :

a- Approximations in the theoretical analysis, and

b- Experimental errors.

These are discussed in turn below.

4.3.1 Factors affecting the Theoretical Results

1- Effect of geometric parameters

The equation proposed for the critical buckling stress, Eqn.(46), is a function of tangent modulus (E_t), mean radius (R) of the cylinder, and the thickness (t) of the tube wall. Since E_t is determined by employing the (R/t) ratio, as was explained in Chapter-3, (R/t) ratio is then a critical parameter for the buckling stress equation. Both of these geometrical parameters may vary in θ or/and Z directions of the tube depending upon the precision of machining. On the other hand, measuring accuracy is another problem. Any variations in these dimensions effects the buckling stress considerably since the stress is inversely proportional with the square of the (R/t) ratio.

a- Mean Radius

The mean radii of the tubes were found to be varying from 18.7 mm to 19.4 mm for copper and from 16.94 mm

to 17.01 mm for brass specimens as shown in Table-2. These are the mean values of the radii measured at different sections of the tubes. The inaccuracies in these dimensions due to machining or measuring errors were found to be not greater than 0.05 mm, depending upon the device used. Therefore the possible inaccurate value of R will not change the R/t ratio appreciably. Take, for instance, the specimen-1. If the radius is measured 0.05 mm smaller than the actual and substituted into Eqn.(46), buckling stress decreases by 0.013 percent.

b- Thickness

Though the sensitivity of the R/t ratio to R values is small, it is highly sensitive to the value of the thickness t; as the thickness of the specimens used in the experiments were smaller than 1 mm. Therefore a variation in this dimension will effect the buckling stress considerably. For example, substitution of a thickness value into the buckling equation 0.05 mm smaller than the actual value will result in 2.28 % decrease in the calculated buckling stress for specimen-1.

The change in thickness along the circumference seldom occurs but is probable along the tube length due to machining inaccuracy. Since buckling failure starts at the thinnest part of the cylinder wall, then the minimum thickness value must be found and substituted into the proposed equation for the theoretical and experimental values to be comparable.

2- Assumption on effective length

Going back to Figs.9 and 10 of Chapter-3, the effective length employed in the theoretical results was determined from the development of the ellipse. A segment of the ellipse and the 45° helix were assumed to

be coincident for the length termed as m-n.

Obviously the two curves are coincident at one point only (point A in Fig.10). The tangents are no longer common when moved away from this point. However, as an initial assumption for the theoretical work, the deviation between the tangents was ignored up to a value of 1^{o}. In other words, the tangent at point A was assumed to be common until the points m and n which were defined by substituting 1^{o} for γ in equation (22). Comparison between the theoretical and experimental results shows that the error involved due to this assumption is negligibly small for practical purposes. However, substitution of 0.95^{o} in the said equation yields a closer result (See Table-5). Therefore it is suggested to modify the theoretical equation as follows based on the experimental results.

3- Approximation of the development of the ellipse by a parabola

In order to facilitate the derivation of a simple equation to predict plastic buckling of a tubular element, the development of the ellipse, obtained by the intersection of the cylinder with a 45^{o} plane, was approximated by a parabola along the effective length. The error involved due to this assumption was found to be about 0.15 %. The analysis pertinent to this error is presented in Appendix-B of the thesis.

4- Approximation by Swift's Expression

The experimental stress-strain curve was converted to true stress-true strain curve and then the resulting curve was approximated by Swift's expression.

Though Swift's expression is a close approximation of the actual true stress-true strain curve, a perfect fit is impossible. By a suitable computer programming,

TABLE-5 Percent errors between theoretical and experimental results for different γ values

Specimen		Percent Errors		
		$\gamma = 1^{o}$	$\gamma = 0.95^{o}$	$\gamma = 0.8^{o}$
COPPER	A_1	- 0.077	+ 1.025	+ 4.13
	A_2	+ 1.40	+ 2.30	+ 5.24
	A_3	- 3.93	- 2.30	+ 1.00
	A_4	+ 0.94	+ 2.43	+ 4.96
	B_1	+ 2.18	+ 2.25	+ 2.85
	B_2	+ 2.45	+ 2.58	+ 1.85
	B_3	+ 1.63	+ 1.81	+ 1.70
	C_1	+ 0.41	+ 2.40	+ 6.72
	C_2	+ 2.21	+ 3.50	+ 7.20
BRASS	D_1	- 4.01	- 2.90	+ 1.72
	D_2	- 3.21	- 1.50	+ 2.96
	D_3	- 3.54	- 2.57	+ 2.03
	D_4	- 4.81	- 3.59	+ 1.00

experimental points were compared with the points obtained from the Swift's equation. The computer results appended to the thesis shows that, at certain points on the curve, there may be an error. Therefore if the critical buckling stress is at a value where the analytical expression does not fit the actual curve accurately, critical stress predicted by the buckling equation will naturally deviate from the experimental result.

Fortunately this error reflects to the E_t - R/t curve at a smaller magnitude. However, all workers investigating plastic buckling should be conscious of this fact and must check the degree of agreement between the true stress-true strain curve and the analytical expression for the plastic curve.

5- Anomalous effects

One of the assumptions made in the theoretical analysis was the uniformity of stress acting on the section of the tube. Though this is a permissible approximation in calculating the torque resistance of thin tabular cylindrical members, in actual case, the shear stress, no matter how slight, varies across the section. Consequently, it may be said that a certain amount of error creeps into theoretical analyses due to this assumption. The magnitude of error involved increases with the increase in thickness t.

The material parameter E_t is known to be anisotropic for parts which are produced by heavy rolling. In the theoretical analysis, E_t value was determined from the specimens machined in the axial direction. However, the buckling element of the tube is aligned at 45^o with the longitudinal axis. If a material exhibits directionality, the actual value of E_t must be determined accordingly.

Cutting specimens from the tubes in the direction of buckling was practically impossible. However, to gain an insight to the error involved, a microscopic examination was done. The results of the microscopic examination revealed heavy directionality for copper tubes as shown in Fig.(29). The effect was not so pronounced in brass specimens, in Fig.(30). From relevant studies on anisotropy of sheet materials [27], for heavily rolled copper sheets, the Young's modulus measured at 45^{o} to the rolling axis has been shown to be about 80 % of the nominal value. This explains why the theoretical results obtained for copper tubes overestimated the actual buckling stress. Since no appreciable directionality was observed for brass specimens, the theoretical results are consistently below the experimental values.

The simplified principal stress equation (Eqn.19 in Chapter-3) for thin cylinders ignors the polar moment of inertia term in the classical shear stress equation for torsion. For thin cylinders the simplifying assumption is accepted not to cause appreciable error. However, undoubtedly this simplifying assumption is also responsible for the deviation between the theoretical and experimental results.

4.3.2 Factors affecting the experimental results

1- Loading

The experimental results are sensitive to end conditions during loading as well. Though great care was exercised to apply pure torsion to the specimens, it was impossible to eliminate some of the insidious effects. According to Saint Venànt's theory, the end conditions do not influence the character of loading at points beyond a distance which is greater than the maximum cross-sectional dimension of the specimen. In this work the pure torsion

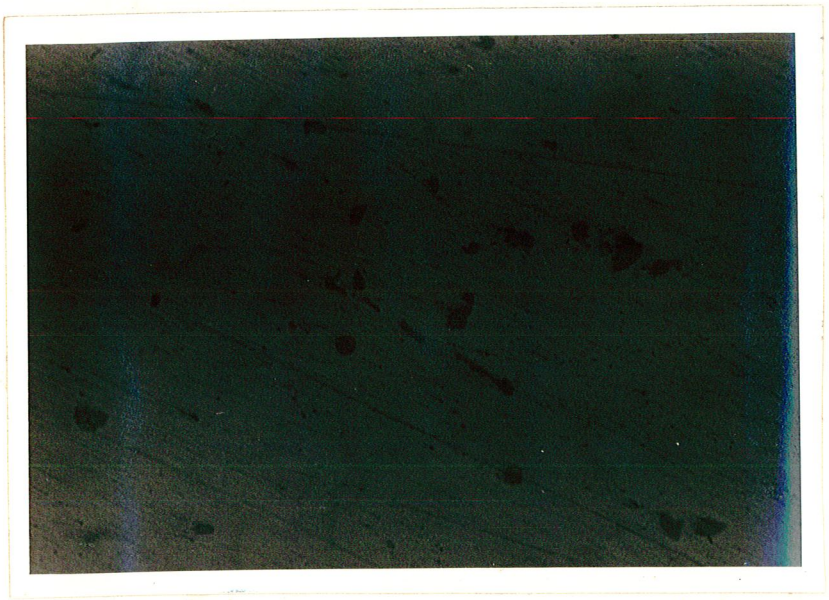

(a)

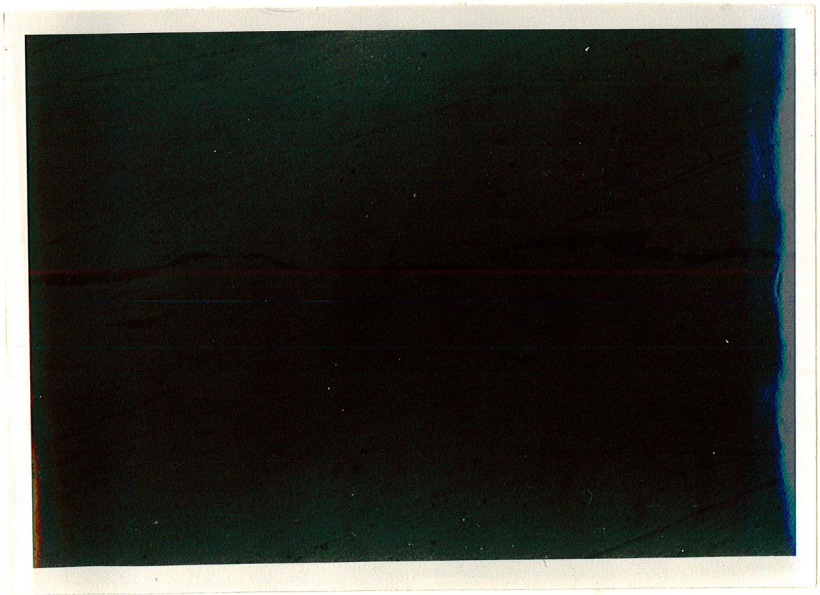

(b)

Fig. 29 Microscopic examination of copper specimens;

(a) on transverse cross section,

(b) on longitudinal cross section.

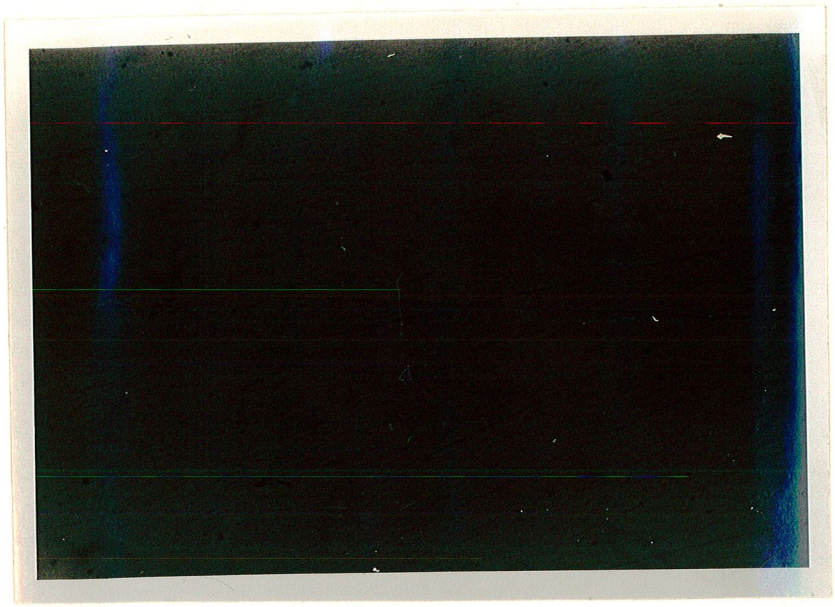

(a)

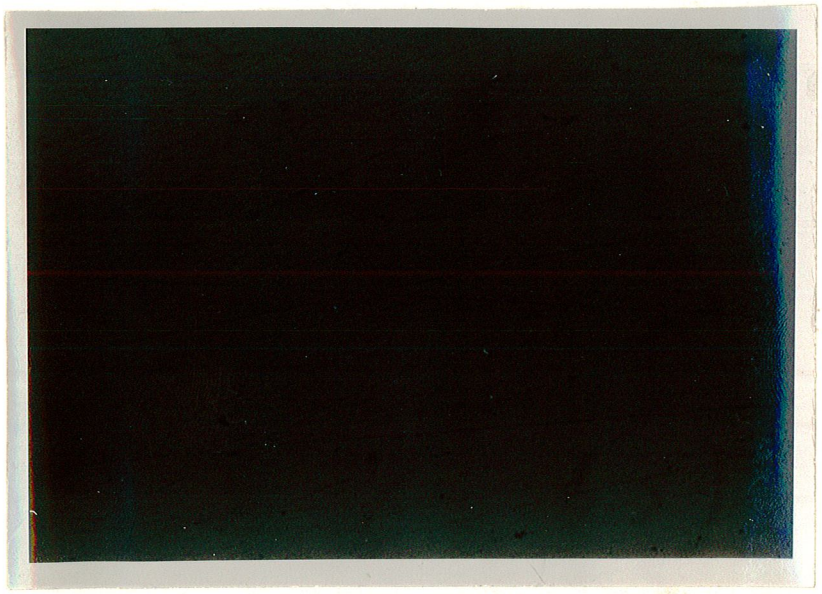

(b)

Fig. 30 Microscopic examination of brass specimens

(a) on transverse cross section,

(b) on longitudinal cross section.

exists only in the mid-portion of the cylinder equal in length to $L'-2R$; where L' is the distance between the plugs. Consequently, for short specimens more irregular results were obtained as compared with the longer specimens.

True stress-true strain curves of the materials used in the experiments were obtained by replotting the experimental tensile curves. These curves were later converted to analytical expressions by employing Swift's equation. The tangent moduli were determined at various points on the plastic curve by differentiating the analytical expression, Eqn.(48). The values thus obtained were substituted into the proposed buckling stress equation and the corresponding R/t values were determined. Finally these R/t values were plotted against E_t. Thus for a given specimen, i.e., R/t value, this graph was used to determine the corresponding E_t value. When the given R/t and thus determined E_t values were substituted into the critical stress equation, the buckling stress was hence obtained.

Obviously, depending upon the size of the graph, the E_t value corresponding to the given R/t value is subject to a certain amount of error. For example, if the tangent modulus is read 100 kg/mm^2 higher than the actual, based on the data for specimen-1, the error involved is about 2.07 %.

Employing a curve for this purpose is a great expedient. However, it is subject to reading errors as outlined. An attempt was therefore made to express these curves analytically. From the log-log plot, the curves, as numbered in Fig.(31), can be expressed analytically as follows :

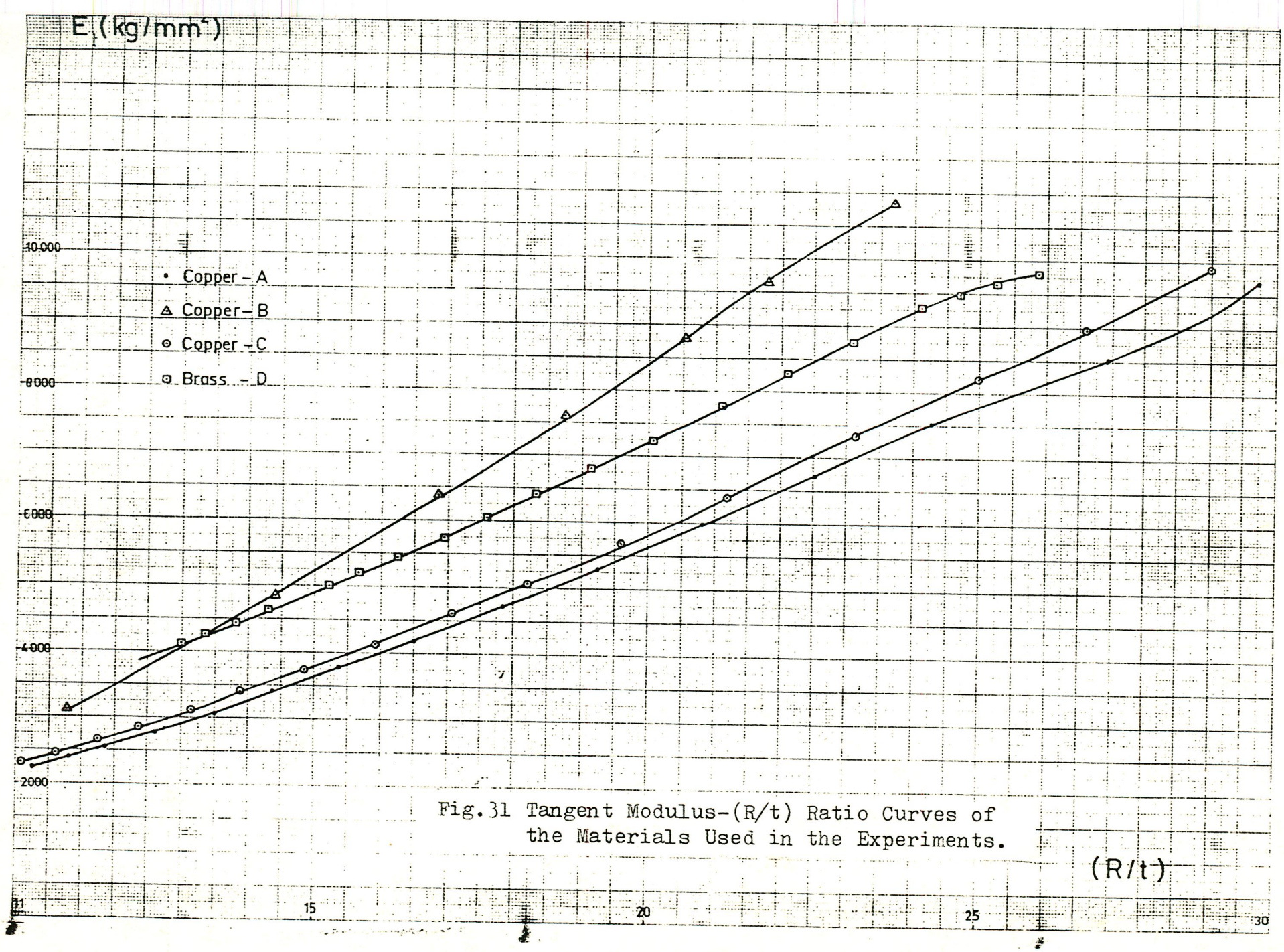

Fig.31 Tangent Modulus-(R/t) Ratio Curves of the Materials Used in the Experiments.

Material	Equations
A	$E_t = 54.2412(R/t)^{1.55}$
B	$E_t = 39.163(R/t)^{1.567}$
C	$E_t = 40.845(R/t)^{1.7674}$
D	$E_t = 124.2(R/t)^{1.3462}$

Within the region of interest, the values of E_t corresponding to various R/t ratios were checked with the values from the graph. It was seen that the differences were negligibly small.

4.4. Conclusions

Plastic buckling equation of thin walled circular cylinders is determined by considering the buckled part of the cylinder as a fixed-ended curved column and by applying the well known Euler buckling formula with some modifications.

Plasticity is introduced into this equation simply by replacing the Young's modulus by the tangent modulus. The resulting equation satisfies the actual conditions of thin walled cylinders under torsional loading. Thus, a simple tension test is all that is required to determine the material parameter (E_t) of the given equation, since the other parameters, i.e., R and t, are known for a given tube.

By comparing the results from the proposed equation and the experiments, the following results are concluded:

1- The proposed equation satisfies the experimental values quite well (maximum error is 3.93 %) for the thin walled circular cylinders of finite length.

2- The deviation between the theoretical and the experimental results increases due to the end disturbances as the length of the tube decreases (See Table-3).

3- Both material (E_t) and geometrical (R and t) parameters must be determined accurately to obtain consistent results.

4- The tube material should be ductile and its mechanical properties in tension and compression must be equal to employ the proposed equation; or else its compressive properties must also be determined.

CHAPTER 5

SUGGESTED EXTENSION OF THE WORK DONE

An interesting extension of the work done could be to study the plastic torsional buckling of thin walled tubes based on the deformation of plastic hinges.

Though this method wouldn't yield a simple solution as compared with the selected approach, it would be of academic interest.

The plastic buckling phenomenon can be approximated to an equivalent system of deformation in which plastic and to elasto-plastic hinges are assumed to form. The external energy expended to bend these hinges is the applied torque.

The success of this approach would depend upon how well the limit analysis, pertinent to the geometry, could be carried out. It is necessary to determine in which parts of the hinges of the tube must form to effect instability.

This analysis must then be combined with an equilibrium study to determine what external loads are needed to exceed the resistance of the material at hinges.

Equations exist for elasto-plastic and plastic hinges in the relevant literature [28] . However, these equations are based on the assumption that the material is elastic and fully plastic. Obviously these equations must be modified to represent the real behaviour of the materials which exhibit work hardening.

An attempt was also made to determine the possible hinge points on the deformed specimen. This is illustrated in Fig.32. This figure is based on the analysis of the deformed specimen. If the cross section of the

deformed tube, cut by 45° plane, is examined, for points under large deformation will be observed (Fig.32). Hence the real situation may be approximated to a deformation consisting of :

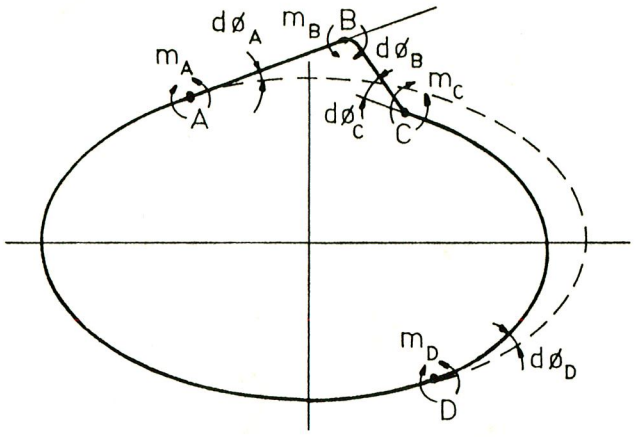

Fig.32 Equivalent hinge deformation of the tube cross section cut by 45° plane.

Case 1 : two plastic hinges at points B and C, and two elastic-plastic hinges at points A and D,

Case 2 : three plastic hinges at points B, C and D, one elastic-plastic hinge at point A,

and the portions between which are assumed to be rigid.

Though this geometric analysis sounds feasible, the exact worth of this reasoning can not be evaluated without a detailed limit analysis based on energy balance. It's felt that an alternative solution could be put forward by a detailed limit analysis. However, such an analysis would be rather detailed and wouldn't be as practicle as approach assumed in this thesis.

LIST OF REFERENCES

1 - ARON, G., "Das Gleichgewicht and die Bewegung Einer Unendlich Dünnen, Belicbig Gekrummten, Elastichen Schale" , Jour. für Reine und Ang. Math., 78, 1874.

2 - LOVE, A.E.H., "On the Small Free Vibrations and Deformations of Thin Elastic Shells", Phil. Trans. Roy. Soc., 179 (A), 1888.

3 - KIRCHOFF, G., "Vorlesungen Über Mathematische Physik", Vol.1, Mechanik, 1876.

4 - FLÜGGE, W., "Die Stabilitat der Kreiszylinderschale", Ingenieur-Archiv, Vol.3, December, 1932, p.463.

5 - FLÜGGE, W., "Statik and Dynamik der Schalen", Julius Springer, Berlin, Germany, 1934, p.118.

6 - BIENZO, C.B., and GRAMMEL, R., "Technische Dynamik", Julius Springer, Berlin, Germany, 1939, p.469.

7 - TIMOSHENKO, S., "Theory of Plates and Shells", McGraw Hill Book Company, Inc. New York, N.Y., 1940, p.440.

8 - DONNELL, L.H., "Stability of Thin Walled Tubes Under Torsion", NACA Rep. 479, Washington, D.C., 1933.

9 - DONNELL, L.H., "Beams, Plates and Shells", McGraw Hill, New York, 1976.

10- BRUSH, D.O., and ALMROTH, B.O., "Buckling of Bars, Plates, and Shells", McGraw Hill, New York, 1975.

11- TIMOSHENKO, S., "Theory of Elastic Stability", McGraw Hill Book Company, New York, 1936.

12- JOHNSTON, B.G., "Guide to Stability Design Criteria for Metal Structures", John Wiley and Sons Inc., New York, 1976.

13- BATDORF, S.B., "A Simplified Method of Elastic Stability Analysis for Thin Cylindrical Shells", NACA Rep. 874, 1947.

14- FLÜGGE, W., "Stresses in Shells", Springer - Verlag, New York, 1973.

15- Buckling of Thin - Walled Circular Cylinders, NASA SP - 8007, 1968.

16- BAKER, E.H., KOVALEVSKY, L., and RISH, F.L., "Structural Analysis of Shells", McGraw Hill, New York, 1972.

17- BAKER, E.H., CAPELLI, A.P., KOVALEVSKY, L., RISH, F.L., and VERETTE, R.M., "Shell Analysis Manual", NASA CR 912, 1968.

18- FOSTER, C.G., "Interaction of Buckling Modes in Thin-Walled Cylinders", Exp.Mech. March, 1981.

19- REES, D.W.A., "Plastic Torsional Buckling of Thin-Walled Cylinders", Jour.Appl.Mech., Vol.49, pp:663-666, Sept.1982.

20- BATDORF, S.B., STEIN, M., and SCHILDCROUT, M., "Critical Stress of Thin-Walled Cylinder in Torsion", NACA TN, 1344, (1947).

21- BLEICH, F., "Buckling Strength of Metal Structures". McGraw Hill, New York, 1952.

22- DRUCKER, D.C., "Introduction to Mechanics of Deformable Solids", McGraw Hill Book Co., New York, 1967.

23- CHAJES, A., "Principles of Structural Stability Theory", Prentice Hall Inc. Englewood Cliffs, N.J., 1974.

24- SEELY, F.B., and SMITH, J.O., "Resistance of Materials", John Wiley and Sons, Inc., 1958.

25- ENGESSER, F., "Ueber die Knickfestigkeit Gerader Stäbe", Z.Architekt. Ing., Vol.35, p.455, 1889.

26- SIVACI, K., and KAFTANOĞLU, B., "Yüksek Sıcaklıklarda Çelik, Pirinç, Bakır ve Alüminyum Malzemelerinin Plastik Özelliklerinin Bulunması", TBTAK Yayınları, No.296, MAG Seri No : 30, 1975.

27- WEERTZ, J., "Elasticity of Copper Sheet", Z.Metallkunde, Vol.25, pp.101-103, 1931.

28- JOHNSON, W., and MELLOR, P.B., "Engineering Plasticity", Van Nostrand Reinhold Company Ltd., Molly Millar's Lane Wokingham, Berkshire, 1975.

29- FOX, L.R., "Optimization Methods for Engineering Design", Addison Wesley, 1971.

APPENDICES

APPENDIX-A

DETERMINATION OF THE EQUATION FOR THE DEVELOPMENT OF AN ELLIPSE

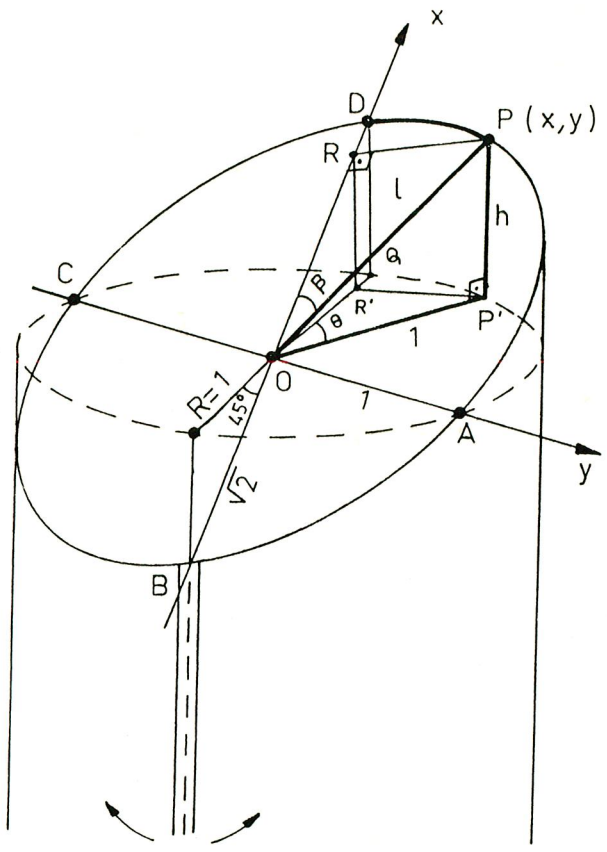

Fig. A

Equation of an ellipse is

$$\frac{x^2}{a^2} + \frac{y^2}{b^2} = 1 \qquad (1)$$

As in this analysis the ellipse is formed by the intersection of the tube with a 45° plane, substituting b=1, and a=1/sin 45 (Fig. A) into Eqn.(1) gives

$$\frac{x^2}{2} + y^2 = 1 \qquad (2)$$

From triangle OPR

$$x^2 + y^2 = 1^2 \qquad (3)$$

and from Eqns. (2) and (3)

$$x = \sqrt{2}\sqrt{l^2 - 1} \tag{4}$$

From the figure

$$\cos\beta = \frac{x}{l} \tag{5}$$

Substituting Eqn. (4) into Eqn. (5) and solving for l

$$l^2 = \frac{2}{2-\cos^2\beta} \tag{6}$$

From triangle OP'P

$$l^2 = 1 + h^2$$
$$h^2 = l^2 - 1 \tag{7}$$

Substituting Eqn. (6) into Eqn. (7) gives

$$h^2 = \frac{\cos^2\beta}{1+\sin^2\beta} \tag{8}$$

On the other hand,

$$\sin\beta = \frac{y}{l} \tag{9}$$

and

$$\sin\theta = \frac{y}{l} \tag{10}$$

From Eqns. (9) and (10),

$$l = \frac{\sin\theta}{\sin\beta} \tag{11}$$

or

$$l^2 = \frac{\sin^2\theta}{\sin^2\beta} \tag{12}$$

Equating Eqns. (6) and (12) give the relationship between β and θ as

$$\sin^2\theta = \frac{2\sin^2\beta}{2-\cos^2\beta} \tag{13}$$

or

$$\sin^2\beta = \frac{\sin^2\theta}{1+\cos^2\theta} \tag{14}$$

using the trigonometric relationships

$$\cos^2\beta = 1 - \sin^2\beta$$

$$\sin^2\theta = 1 - \cos^2\theta$$

Eqn. (8) can be written as

$$h^2 = \frac{1-\sin^2\beta}{1+\sin^2\beta} = \frac{1-(1-\cos^2\theta)/(1+\cos^2\theta)}{1\ (1-\cos^2\theta)/(1+\cos^2\theta)}$$

$$= \frac{1+\cos^2\theta - 1+\cos^2\theta}{1+\cos^2\theta + 1-\cos^2\theta} = \frac{2\cos^2\theta}{2} = \cos^2\theta$$

which consequently yields

$$h = \cos\theta \qquad (15)$$

APPENDIX-B

B-1 DETERMINATION OF THE ARC LENGTH OF AN ELLIPSE

The development of an ellipse (cosine curve) may be approximated by a parabola (Fig.B)for the critical section. The equation of the parabola is

$$h = -\frac{4}{\pi^2}\left(\theta^2 - \frac{\pi^2}{4}\right) \tag{16}$$

for the interval $-\frac{\pi}{2} \leqslant \theta \leqslant \frac{\pi}{2}$.

Arc length of Eqn. (16) for any point in the interval $0 \leqslant \theta \leqslant \frac{\pi}{2}$ can be calculated from

$$S = \int_0^{\theta} \sqrt{1+(dh/d\theta)^2}\, d\theta \tag{17}$$

Differentiating Eqn. (16) with respect to θ first and then substituting into Eqn. (17) yields

$$S = \int_0^{\theta} \sqrt{1+\left(-\frac{8\theta}{\pi^2}\right)^2}\, d\theta \tag{18}$$

Letting $U = \frac{8\theta}{\pi^2}$, Eqn. (18) becomes

$$S = \frac{\pi^2}{8}\int_0^{u} \sqrt{1+u^2}\, du \tag{19}$$

Integrating Eqn. (19) yields

$$S = \frac{\pi^2}{8}\left[\frac{u\sqrt{1+u^2}}{2} + \frac{1}{2}\ln\left(u+\sqrt{1+u^2}\right)\right] \tag{20}$$

B-2 ERROR ANALYSIS

Peripherial length of an ellipse is

$$P = 2\pi\sqrt{\frac{1}{2}\left(a^2+b^2\right)} \tag{21}$$

Since b=1 and a = 1/sin 45, Eqn. (21) then gives

$$P = 7.6953 \tag{22}$$

Consequently, the arc length of the quarter of an

ellipse of unit minor axis cut from a cylinder by a 45^{o} plane is

$$\frac{P}{4} = 1.9238 \tag{23}$$

However, the arc length of a quarter ellipse, for $\theta=\frac{\pi}{2}$ and as calculated from Eqn. (20) is

$$S = 1.92667 \tag{24}$$

Thus, the error introduced over the total length of a quarter ellipse is

$$\%\varepsilon = \frac{1.92667 - 1.9238}{1.9238} \times 100 = 0.1492\%$$

Obviously the error will be smaller for the arc lengths smaller than the length of the quarter ellipse.

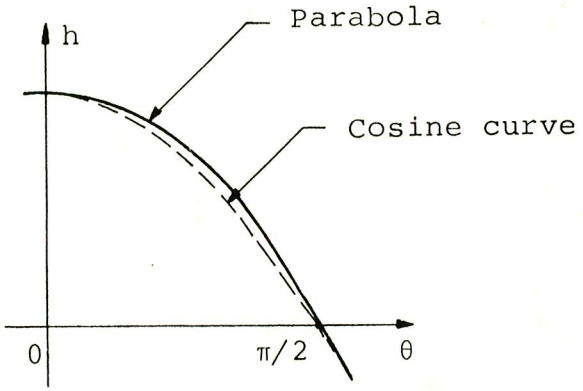

Fig. B

APPENDIX - C

DETERMINATION OF THE THICKNESS OF AN ELLIPSE CUT FROM A THIN WALLED TUBE

The equation of an ellipse in rectangular coordinate system is

$$\frac{x^2}{a^2} + \frac{y^2}{b^2} = 1 \tag{25}$$

or in polar coordinate

$$\frac{r^2\cos^2\beta}{a^2} + \frac{r^2\sin^2\beta}{b^2} = 1 \tag{26}$$

Substituting $\cos^2\beta = 1 - \sin^2\beta$ into Eqn.(26) and re-arranging gives

$$r = \frac{ab}{\sqrt{b^2+(a^2-b^2)\sin^2\beta}} \tag{27}$$

But $a^2 = (b/\sin 45)^2 = 2b^2$, Eqn.(27) becomes

$$r = \frac{a}{\sqrt{1+\sin^2\beta}} \tag{28}$$

Consider the ellipse shown in Fig. C is formed by cutting a thin-walled cylinder by a 45^o plane. Designating the inner and outer ellipses by subscripts i and o, respectively, the dimension t' (Fig.C) at any point can be calculated from

$$t' = r_o - r_i = \frac{a_o}{\sqrt{1+\sin^2\beta}} - \frac{a_i}{\sqrt{1+\sin^2\beta}}$$

$$t' = \frac{1}{\sqrt{1+\sin^2\beta}}(a_o - a_i) \tag{29}$$

From Fig. C

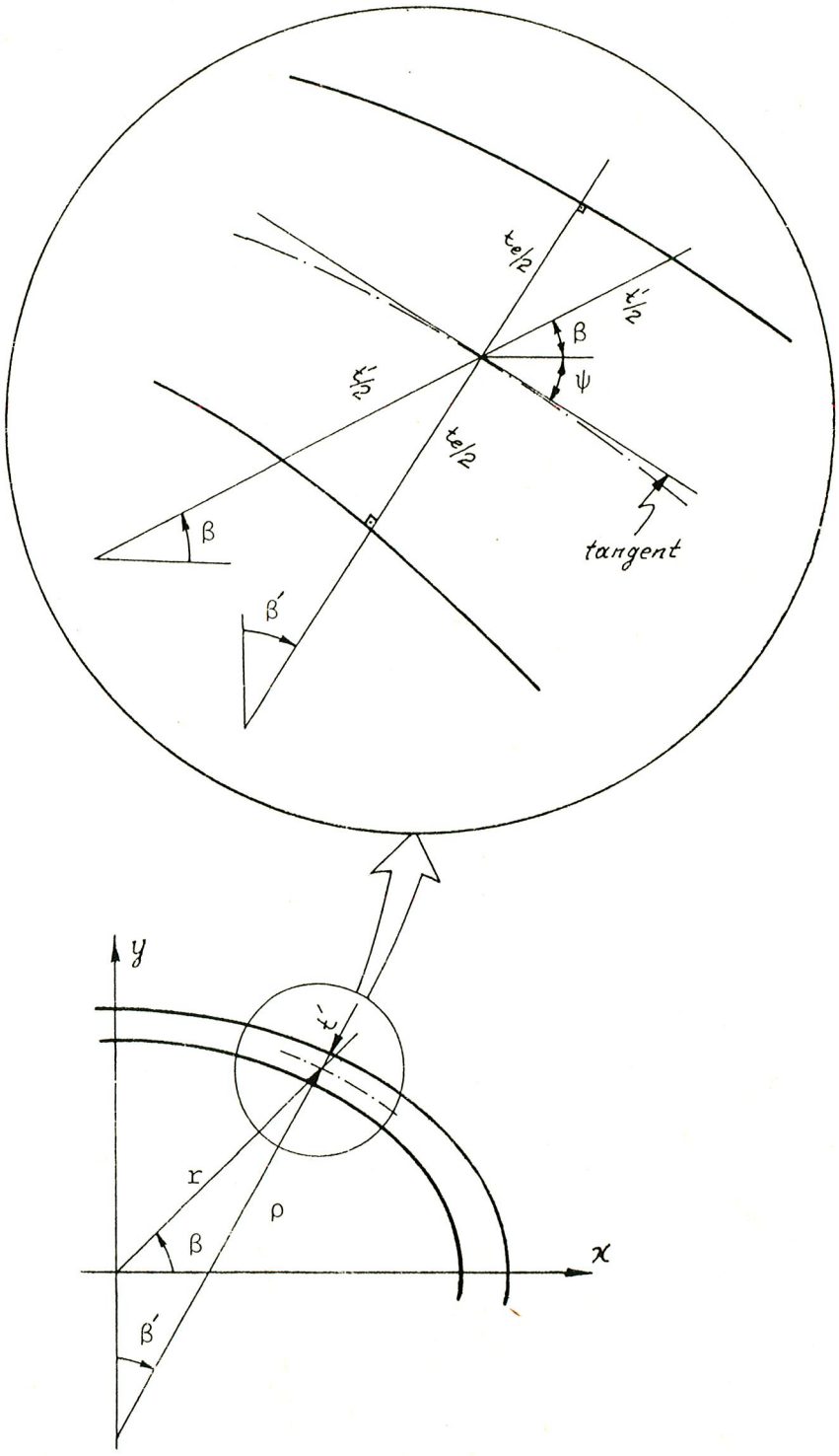

Fig.C

$$-\frac{dy}{dx} = \tan\psi \tag{30}$$

From Eqn. (25)

$$y = b\sqrt{1-x^2/a^2} \tag{31}$$

Differentiating Eqn. (31)

$$\frac{dy}{dx} = -\frac{b}{a^2}\frac{x}{\sqrt{1-x^2/a^2}} \tag{32}$$

From Eqns. (30) and (32)

$$\tan\psi = \frac{b}{a^2}\frac{x}{\sqrt{1-x^2/a^2}} \tag{33}$$

or in polar coordinates

$$\tan\psi = \frac{b}{a^2}\frac{r\cos\beta}{\sqrt{1-\frac{r^2\cos^2\beta}{a^2}}} \tag{34}$$

re-arranging Eqn. (34)

$$\tan\psi = \frac{b}{a^2}\frac{\cos\beta}{\sqrt{\frac{1}{r^2}-\frac{\cos^2\beta}{a^2}}} \tag{35}$$

From Eqn. (26)

$$\frac{1}{r^2} = \frac{\cos^2\beta}{a^2} + \frac{\sin^2\beta}{b^2} \tag{36}$$

Substituting Eqn. (36) and $a^2 = 2b^2$ into Eqn. (35) and simplifying

$$\tan\psi = \frac{\cot\beta}{2} \tag{37}$$

or

$$\psi = \tan^{-1}\left(\frac{\cot\beta}{2}\right) \tag{38}$$

From Fig. (C)

$$t_e = t'\sin(|\psi| + \beta) \tag{39}$$

APPENDIX-D

TENSOMETER

Tension tests were conducted by a MONSANTO tensometer (Fig.D1) which can also be used for shear, compression, and bend tests. Force is applied to the specimen by the spring beams ranging from 31.5 kg to 2000 kg, the latter being the maximum load of the machine for each type of test.

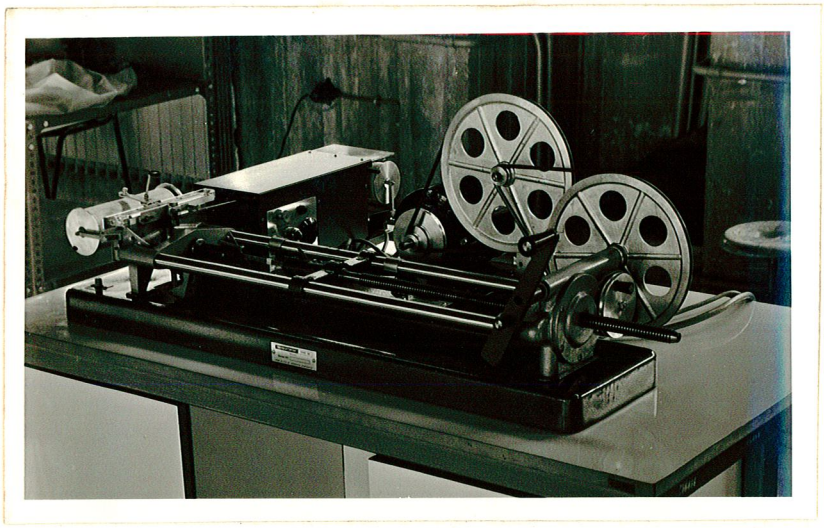

Fig.D1

A hand or motor driven gear box of high mechanical advantage applies the force to the test piece held in chucks. The force deflects the spring beam and this deflection operates a level acting on a piston in a cylinder containing mercury-driving mercury up to a glass tube which is calibrated to show the applied force with respect to beam deflection.

Although in most circumstances hand operation is usually used, the machine,can be motor driven (Fig.D1)

when a constant rate of extension is essential or where materials with usually large extensions have to be tested. Force-elongation graph can be plotted either by puncturing the graph paper with a manually operated cursor or by an automatic recorder when tests made at high speeds or when forces change rapidly (Fig. D2).

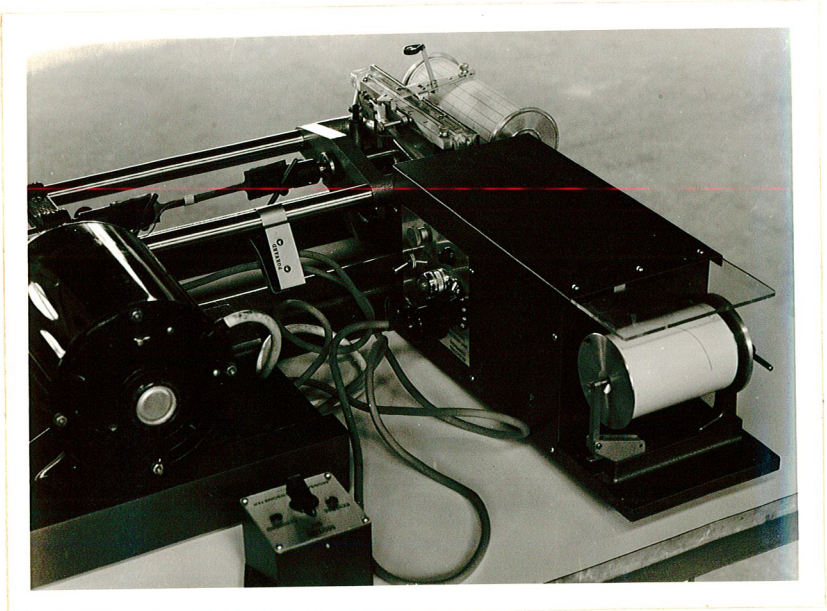

Fig. D2

The recording graph is mounted on a cylindrical drum connected directly to the main drive. The drum-drive has three alternative gear ratios and thus the magnification of elongation may be varied between 16:1, 8:1,, and 4:1.

The overall dimensions of the machine are as follows :

Length : 965 mm
Height : 230 mm
Width : 235 mm.

APPENDIX-E

COMPUTER PROGRAM FOR THE EVALUATION OF TENSION TESTS

```
      DIMENSION DEL(100),STRESS(100),STRAIN(100),EQST(100)
     1,EQSTR(100),
     2EL(100),FL(100),FORCE(100),FARK(100),B(500),F(500)
     3,SUMA(100),
     4SUMB(100),SUMEN(100),SEL(100),AL(100),EQT(100)
     5,EQR(100),SAL(100)
      DIMENSION S(100),SS(100),X(100),Y(100),ST(100)
     1,EST(100),DY(100)
     2,DIFF(200),EN(100),DX(100),SM(100),ERROR(200),STRT(100)
     3,TANMOD(50),BEPS(50),TM(50),SR(50),RTTR(50)
C     DEL(I) IS THE HORIZONTAL DISTANCE OF A POINT OF THE
C     FORCE-EXTENSION CURVE ON THE TENSOMETER GRAPH PAPER
C     C IS THE EQUATION OF THE CHARACTERITICS CURVE OF
C     THE SPRING BEAM USED
C     ELC IS THE CONSTANT IN THE PROPOSED EQUATION FOR
C     R/T RATIO
      READ(5,2) N,AREA,BOY,YM,C,ELC,FOR,L
    2 FORMAT(I3,F7.4,F6.2,F8.2,F7.5,F11.9,F6.2,I2)
      READ(5,1)(DEL(I),I=1,N)
    1 FORMAT(10F7.3)
      WRITE(6,3)L
    3 FORMAT(20X,'DATA NO=',I2,/)
      VOL=BOY*AREA
      AKAT=0.0625
      SM(1)=0.
      SM(2)=0.
      EQST(1)=0.
      WRITE(6,4)
    4 FORMAT(25X,'I',12X,'X',12X,'Y',10X,'EN',9X,'SM'/,
     124X,55('-'))
      DO 5 I=1,N
      FORCE(I)=FOR+I*2.5
      STRESS(I)=FORCE(I)/AREA
      FARK(I)=C*FORCE(I)
      EL(I)=DEL(I)-FARK(I)
      SEL(I)=AKAT*EL(I)
      STRAIN(I)=SEL(I)/BOY
      SS(I)=1+STRAIN(I)
      EQST(I)=STRESS(I)*SS(I)/1000.
      EQSTR(I)=ALOG(SS(I))
C     DETERMINATION OF THE CONSTANTS OF LUDWIK'S  EXPRESSION
      IF(I.EQ.1) GO TO 5
      X(I)=ALOG(EQST(I))
      Y(I)=ALOG(EQSTR(I))
      IF(I.LT.3) GO TO 5
```

```
      DY(I)=Y(I)-Y(2)
      DX(I)=X(I)-X(2)
      EN(I)=DY(I)/DX(I)
      SM(I)=SM(I-1)+EN(I)
      WRITE(6,6) I,X(I),Y(I),EN(I),SM(I)
    5 CONTINUE
      WRITE(6,7)(I,FORCE(I),STRESS(I),EQST(I)
     1,STRAIN(I),EQSTR(I),I=1,N)
    7 FORMAT(25X,'I',1X,'FORCE(I)',2X,'STRESS(I)',4X,
     1'EQST(I)',5X,'STRAIN(I)',6X,'EQSTR(I)',/,24X,64('-'),/
     2,(23X,I3,2X,F6.2,3X,F9.6,1X,F11.6,2X,E13.6,1X,E13.6))
    6 FORMAT(23X,I3,6X,F11.7,2X,F11.7,2X,F9.7,2X,F9.7)
      NS=N
      L=2
      M=NS/2
      N=NS-1
      ENL=SM(NS)/(NS-2)
      SAL(1)=0.
      DO 8 K=2,NS
      ST(K)=EQSTR(K)**ENL
      AL(K)=EQST(K)/ST(K)
      NN=K-1
      SAL(K)=SAL(NN)+AL(K)
    8 CONTINUE
      NK=K-1
      AL1=SAL(NK)/(NK)
      DO 9 J=2,NS
      EST(J)=AL1*ST(J)
      DIFF(J)=EQST(J)-EST(J)
      ERROR(J)=(DIFF(J)/EQST(J))*100
    9 CONTINUE
      WRITE(6,10) (J,EST(J),EQST(J),DIFF(J),ERROR(J),J=2,NS)
   10 FORMAT(25X,'J',4X,'EST',8X,'EQST',9X,'DIFF',7X,'ERROR',
     1/,24X,50('-'),/,(23X,I3,2X,E8.2,3X,E8.2,5X,E8.2,2X,E11.5))
C     CONSTANTS OF LUDWIK'S EXPRESSION
      WRITE(6,11)ENL,AL1
   11 FORMAT(25X,'VALUES OBTAINED USING LUDWIK EXPRESSION',
     1//,25X,'N=',E12.6,5X,'A=',E15.3)
C     PROGRAM FOR CURVE FITTING (SWIFT'S EXPRESSION)
      T=0.1
C     T IS THE INITIAL ASSUMED VALUE FOR EQUATION 13
C     IN REFERENCE 26
      EQML=EQST(M)/EQST(L)
      EQNL=EQST(N)/EQST(L)
      EM=ALOG(EQML)/ALOG(EQNL)
```

```
      KN=1
      B(1)=0.0
      F(1)=((EQSTR(N)/EQSTR(L))**EM)-(EQSTR(M)/EQSTR(L))
      DO 12 I=1,1000
      IF(I.EQ.1) GO TO 12
      B(I)=B(I-1)+0.002/(10.**KN)
      BEPS1=B(I)+EQSTR(L)
      BEPS2=B(I)+EQSTR(M)
      BEPS3=B(I)+EQSTR(N)
      B21=BEPS2/BEPS1
      B31=BEPS3/BEPS1
C     EQUATION 21 OF REF. 27 (B31**EM=B21)
      F(I)=B31**EM-B21
      ORAN=(F(I)-F(I-1))/(F(I)+F(I-1))
      IF(ABS(ORAN).LT.0.000001) GO TO 13
      IF(I.EQ.1) GO TO 12
      IF(F(I).GT.0.0.AND.F(I-1).LT.0.0.OR.F(I).LT.0.0
     *.AND.F(I-1).GT.0.0) GO TO 14
      GO TO 12
   14 KN=KN+1
      F(I)=F(I-1)
      B(I)=B(I-1)
   12 CONTINUE
   13 B1=B(I)
      B1EPSL=B1+EQSTR(L)
      B1EPSM=B1+EQSTR(M)
      B1EPSN=B1+EQSTR(N)
      BNL=B1EPSN/B1EPSL
C     'N' CAN BE FOUND FROM EQN. 22 OF REFERENCE 26
      EN1=ALOG(EQNL)/ALOG(BNL)
C     A CAN BE FOUND FROM SWIFT'S EMPIRICAL FORMULA
      A11=EQST(L)/(B1EPSL**EN1)
      A12=EQST(M)/(B1EPSM**EN1)
      A13=EQST(N)/(B1EPSN**EN1)
      A1=(A11+A12+A13)/3
C     INITIAL VALUES OF CONSTANTS OF SWIFT'S EXPRESSION
      WRITE(6,15)A1,B1,EN1
   15 FORMAT(25X,'A1=',E15.6,5X,'B1=',F10.6,5X,'EN1=',F10.6)
C     NOW CALCULATE THE FINAL VALUES OF A,B,N,USING
C     EQNS.13,15,17 AND 18 OF REF. 26
      AP1=A1/1000.
      SUMA(1)=0.
      SUMB(1)=0.
      SUMEN(1)=0.
      DO 16 I=2,NS
```

```
      EPS11=B1+EQSTR(I)
      BPEN=EPS11**EN1
      BPEN1=EPS11**(EN1-1)
      AEPS=ALOG(EPS11)
      EPS1=EQST(I)-1000*AP1*BPEN
      SUMA(I)=SUMA(I-1)+EPS1*BPEN
      SUMB(I)=SUMB(I-1)+EPS1*BPEN1*AP1*EN1
      SUMEN(I)=SUMEN(I-1)+EPS1*AP1*AEPS*BPEN
   16 CONTINUE
C     GRADIENTS WITH RESPECT TO A,B AND N (EQNS. , ,
C     AND  , IN REF. 27)
      AGRAD=-2000*SUMA(I)
      BGRAD=-2000*SUMB(I)
      ENGRAD=-2000*SUMEN(I)
      CALL TBUL(EQST,EQSTR,NS,AGRAD,BGRAD,ENGRAD,A1,AP1
     1,B1,EN1,T)
      AP2=AP1-T*AGRAD
      B2=B1-T*BGRAD
      EN2=EN1-T*ENGRAD
      IF(ABS(AP2).GT.ABS(B2)) GO TO 17
      IF(ABS(B2).GT.ABS(EN2)) GO TO 18
      GO TO 19
   17 IF(ABS(AP2).GT.ABS(EN2)) GO TO 20
   19 IF(ABS(EN2-EN1).LT.0.00001) GO TO 21
      GO TO 22
   20 IF(ABS(AP2-AP1).LT.0.00001) GO TO 21
      GO TO 22
   18 IF(ABS(B2-B1).LT.0.00001) GO TO 21
   22 AP1=AP2
      B1=B2
      EN1=EN2
      GO TO 20
   21 A2=AP2*1000
      AN2=EN2-1
      WRITE(6,23)
   23 FORMAT(25X,'I',4X,'EQST(I)',5X,'STRT(I)',7X,'DIFF',
     18X,'ERROR',/,23X,52('-'))
      DO 24 I=1,NS
      STRT(I)=A2*((B2+EQSTR(I))**EN2)
      DIFF(I)=ABS(EQST(I)-STRT(I))
      ERROR(I)=(DIFF(I)/EQST(I))*100
      WRITE(6,25) I,EQST(I),STRT(I),DIFF(I),ERROR(I)
      BEPS(I)=B2+EQSTR(I)
      TM(I)=EN2*A2*(BEPS(I)**AN2)
      TANMOD(I)=YM*TM(I)/TM(1)
```

```
      EQST(I)=EQST(I)*1000.
      SR(I)=SQRT(TANMOD(I)/EQST(I))
      RTTR(I)=ELC*SR(I)
   24 CONTINUE
      WRITE(6,26)
   26 FORMAT(25X,'I',8X,'EQST(I)',6X,'TANMOD(I)',10X,
     1'R/I',/,23X,53('-'))
      WRITE(6,27)(I,EQST(I),TANMOD(I),RTTR(I),I=1,NS)
   27 FORMAT(23X,I3,8X,F7.3,4X,E15.7,7X,F8.4)
   25 FORMAT(24X,I3,2X,F9.6,3X,F9.6,3X,F9.6,2X,F11.6)
      WRITE(6,28)A2,B2,EN2
   28 FORMAT(25X,'A=',F6.4,10X,'B=',F8.5,10X,'N=',F8.5)
      STOP
      END
C     ''T' VALUE DETERMINATION USING THE METHOD OF STEEPEST
C     DESCENT WITH LARGE STEP ALGORITHM(REF.29)
      SUBROUTINE TVAL(EQST,EQSTR,NS,AGRAD,BGRAD
     1,ENGRAD,A1,AP1,B1,EN1,T)
      DIMENSION EQST(100),EQSTR(100)
      REAL NORTAK
      ICONT=0
  100 SUMAK=0.
      SUMBK=0.
      SUMNK=0.
      STGAK=0.
      STGBK=0.
      STGNK=0.
      ICONT=ICONT+1
      DO 29 N=1,NS
      AORTAK=AP1-T*AGRAD
      BORTAK=B1-T*BGRAD+EQSTR(N)
      NORTAK=EN1-T*ENGRAD
      BONOR=BORTAK**NORTAK
      ANOR=AORTAK*NORTAK
      ABTK=ALOG(BORTAK)
      AONT1=AORTAK*(NORTAK-1)
      BONT1=BORTAK**(NORTAK-1)
      BONT2=BORTAK**(NORTAK-2)
      BON2T=BORTAK**(2*NORTAK-1)
      BON2T2=BORTAK**(2*NORTAK-2)
      BON2=BORTAK**(2*NORTAK)
      ABGN=AGRAD*BON2
      AA=AORTAK*AORTAK
      AGBT=AGRAD*BONT1
      AGBON=AGRAD*BONOR
```

```
      ABONG=ANOR*BON2T*BGRAD
      ABON=AORTAK*BUNOR
      ORBBG=NORTAK*BONT1*BGRAD
      ABGD=AONT1*BONT2*BGRAD
      AGBD=NORTAK*BUN2T*BGRAD
      AGORB=AGRAD*AORTAK*BON2T
      BOBGR=BUN2T2*BGRAD
      AORBT1=AORTAK*BUNT1
      AORB2T=AORTAK*AORTAK*BON2T
      ORTAK=EQST(N)-1000*AORTAK*BUNOR
C     'SUMAK' MEANS EQN.   40
      SUMAK=SUMAK+ORTAK*BUNOR
      SUMBK=SUMBK+ORTAK*BONT1*ANOR
      SUMNK=SUMNK+ORTAK*AORTAK*ABTK*BUNOR
C     'GAK' MEANS GRADIENT OF A AT'K'TH STEP
      GAK=-2000*SUMAK
      GBK=-2000*SUMBK
      GNK=-2000*SUMNK
      FUNC=GAK*AGRAD+GBK*BGRAD+GNK*ENGRAD
      STGAK=STGAK+(EQST(N)*ORBBG-1000*(ABGN+2*ABONG))
      STGBK=STGBK+(EQST(N)*(AGBT+ABGD)-1000*(2*AGORB
     1+AA*(2*NORTAK-1)*
     2BOBGR))*NORTAK+ENGRAD*(EQST(N)*AORBT1-1000*AORB2T)
      STGNK=STGNK+(EQST(N)*(AGBON+AORTAK*ORBBG)-2000*
     1(AORTAK*ABGN+AA*
     2AGBD))*ABTK+(EQST(N)*AORBT1-1000*AORB2T)*BGRAD
   29 CONTINUE
      TGAK=2000*STGAK
      TGBK=2000*STGBK
      TGNK=2000*STGNK
      TFUNC=TGAK*AGRAD+TGBK*BGRAD+TGNK*ENGRAD
      T1=T-FUNC/TFUNC
      IF(ABS(T-T1).LE.0.000001) GO TO 30
      T=T1
      IF(ICONT.EQ.100) GO TO 31
      GO TO 100
   31 WRITE(6,32)
   32 FORMAT('ICONT IS NOT ENOUGH')
   30 CONTINUE
      RETURN
      END
```